Transgene expression of APOBEC1 causes dysplasia and carcinoma in mouse and rabbit liver due to its aberrant editing of the eukaryotic translation initiation factor 4 gamma 2 (Eif4g2).[20,21] A more striking tumor phenotype is observed in mice with constitutive and ubiquitous AID expression. We previously demonstrated that AID transgenic (Tg) mice developed tumors in various organs, including liver, lung, stomach and lymphoid organs, accompanied by the accumulation of somatic mutations on several tumor-related genes such as *Tp53* and *Myc*.[22,23] Interestingly, we also found that proinflammatory cytokine stimulation induces a substantial upregulation of APOBEC2 transcription *via* the activation of the transcriptional factor nuclear factor-κB (NF-κB) in hepatoma-derived cells, whereas only trace amounts of endogenous APOBEC2 expression are detectable in normal hepatocytes.[24] On the basis of the fact that most human hepatocellular carcinoma (HCC) arises in the setting of chronic liver disease with the features of chronic hepatitis or liver cirrhosis, we hypothesized that APOBEC2 enzyme activity has a role in the accumulation of genetic alterations in tumor-related genes under conditions of hepatic inflammation, thereby contributing to the development of HCC. In this study, we investigated the putative nucleotide editing ability of APOBEC2 on the host genes in hepatocytes, and its relevance to carcinogenesis by establishing Tg mice that constitutively express APOBEC2.

Material and Methods

APOBEC2 Tg mice

Total RNA was extracted from murine liver using Sepasol-RNA 1 Super (Nacalai Tesque, Kyoto, Japan) according to the manufacturer's protocol. Complimentary DNA (cDNA) was synthesized from total RNA with random hexamer primers using a Transcriptor First Strand cDNA Synthesis Kit (Roche, Mannheim, Germany). After amplification of the murine APOBEC2 gene using high-fidelity Phusion Taq polymerase (Finnzymes, Espoo, Finland) with oligonucleotide primers, 5′-GCAGAATTCCACCATGGCTCAGAAGGAAG AGGC-3′(forward) and 5′-ACTCTCGAGCCTACTTCAGGA TGTCTGCC-3′ (reverse), murine APOBEC2 cDNA (1.2 kbp) was cloned downstream of the chicken β-actin (CAG) promoter. The purified fragment of the CAG promoter and APOBEC2 transgene was microinjected into fertilized eggs of the Slc:BDF1, the hybrid of C57BL/6CrSlc and DBA/2CrSlc (Japan SLC, Shizuoka, Japan), to generate APOBEC2 Tg mice. Tg mice were maintained in specific pathogen-free conditions at the Institute of Laboratory Animals of Kyoto University. Control mice were littermates carrying no transgene. Tissue samples from Tg mice were removed and fixed in 4% (w/v) formaldehyde, embedded in paraffin, stained with hematoxylin and eosin and examined for histologic abnormalities. Tissue samples were also frozen immediately in liquid nitrogen for nucleotide extraction. The mice received humane care according to the "Guide for the Care and Use of Laboratory Animals" prepared by the National Academy of Sciences and published by the National Institutes of Health, USA (NIH publication 86-23).

Quantitative real-time reverse transcription PCR

Quantitative real-time reverse-transcription polymerase chain reaction (RT-PCR) for murine *APOBEC1* and *APOBEC2* amplification was performed using a LightCycler® 480 instrument (Roche). cDNA was synthesized from 1 μg of total RNA isolated from the cells with random hexamer primers in a total volume of 20 μL using Transcriptor First Strand cDNA Synthesis Kit (Roche). Real-time PCRs were set up in 20 μL of FastStart Universal SYBR Green (Roche) with the RT product and the following oligonucleotide primers: APOBEC1, 5′-CGAAGCTTATTGGCCAAGGT-3′ (forward) and 5′-AAGGAGATGGGGTGGTATCC-3′ (reverse); APOBEC2, 5′-CCCTTCGAGATTGTCACTGG-3′ (forward) and 5′-TGTTCATCCTCCAGGTAGCC-3′ (reverse). Target cDNAs were normalized to the endogenous RNA levels of the housekeeping reference gene for *18S ribosomal RNA* (*18S rRNA*).[25] For simplicity, the expression levels of *APOBEC2* are represented as relative values compared with the control specimen in each experiment.

Immunoblotting

Homogenates of murine specimens were diluted in 2× sodium dodecyl sulfate sample buffer (62.5 mM Tris-HCl, pH 6.8; 2% SDS; 5% β-mercaptoethanol; 10% glycerol, and 0.002% bromophenol blue) and boiled for 5 min. Protein samples were separated by sodium dodecyl sulfate-polyacrylamide gel electrophoresis on 12% (w/v) polyacrylamide gels and subjected to immunoblotting analysis.[26] A polyclonal antibody against human and murine APOBEC2 was generated using purified recombinant APOBEC2 protein as an immunogen. A mouse monoclonal antibody against α-tubulin was purchased from Calbiochem (San Diego, CA).

Cell culture and transfection

Human hepatoma-derived cell lines HepG2 and Huh7 were maintained in Dulbecco's modified Eagle's medium (Gibco-BRL) containing 10% fetal bovine serum. Trans-IT 293 transfection reagent (Mirus Bio Corporation, Madison, WI) was used for plasmid transfection. To generate stable cell lines, pcDNA3-ERT2 was made by inserting the ERT2 fragment, which was cut out from pERT2[27] with *Bam*HI and *Eco*RI. pcDNA3-APO2-ERT2 was made by inserting the PCR-amplified coding sequence of human *APOBEC2*, which was synthesized by RT-PCR with the oligonucleotide primers 5′-ATAGG TACCATGGCCCAGAAGGAAGAGGC-3′ (forward) and 5′-ATAGGATCCAGCTTCAGGATGTCTGCCAAC-3′ (reverse), into the *KpnI-BamHI* site of pcDNA3-ERT2. HepG2 cells were transfected with a *Sca*I-linearized pcDNA3-APO2-ERT2 vector encoding the active form of APOBEC2 fused with the hormone-binding domain of the human estrogen receptor (ER), designated APOBEC2-ER, and cultured in medium

Cancer Cell Biology

containing G418 (Roche) until colonies of stably transfected clones arose.

Subcloning and sequencing of the target genes

The oligonucleotide primers for the amplification of the human *EIF4G2*, *PTEN*, and *TP53*, and murine *Eif4G2*, *Pten*, *Bcl6* and *Tp53*, genes are shown in Supporting Information Table S1. Amplification of the target sequences was performed using high-fidelity Phusion Taq polymerase (Finnzymes, Espoo, Finland), and the products were subcloned into a pcDNA3 vector (Invitrogen, Carlsbad, CA) using pGEM$^{(R)}$ -T Easy Vector System (Promega, Madison, WI) according to the manufacture's instruction. The resulting plasmids were subjected to sequence analysis as described.[28]

Results

Detection of endogenous APOBEC2 protein expression in hepatocytes

We previously reported that transcription of *APOBEC2* is induced by the proinflammatory cytokine tumor necrosis factor (TNF)-α through the activation of NF-κB. To confirm whether endogenous APOBEC2 protein is elevated in response to TNF-α stimulation in human hepatocytes, we generated a rabbit polyclonal antibody against a common amino-acid sequence to human and murine APOBEC2. Using this anti-APOBEC2 antibody, we first confirmed that plasmid-derived exogenous APOBEC2 protein was efficiently detected by immunoblotting analysis (Fig. 1*a*). We then examined whether endogenous APOBEC2 protein was upregulated by TNF-α stimulation in Huh-7 cells. Immunoblotting analysis using the APOBEC2 antibody revealed that endogenous APOBEC2 protein expression was strongly induced after TNF-α stimulation, suggesting that APOBEC2 protein has a role in hepatocyte function under inflammatory conditions (Fig. 1*b*).

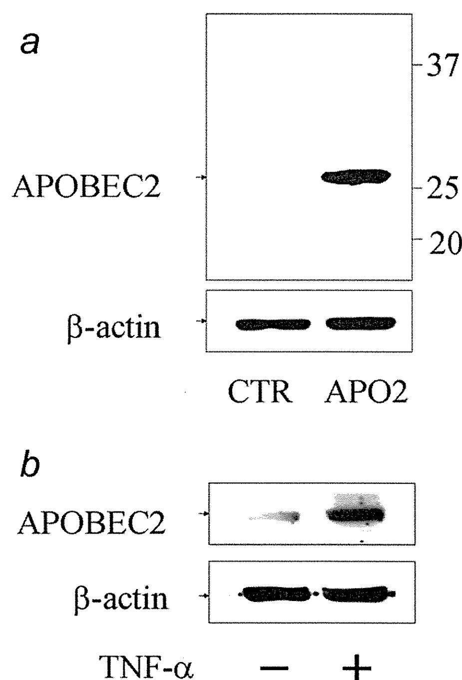

Figure 1. Detection of human APOBEC2 protein in hepatocytes by a specific anti-APOBEC2 antibody. (*a*) Huh7 cells were transfected with plasmid to induce the expression of human APOBEC2 (APO2) or control vector (CTR). After 48 hr, lysates of transfected cells were immunoblotted with anti-APOBEC2 antibody (upper panel) or anti-β-actin antibody (lower panel). (*b*) Huh7 cells were treated with tumor necrosis factor-α (100 ng/ml) for 48 hr followed by immunoblotting using anti-APOBEC2 antibody (upper panel) or anti-β-actin antibody (lower panel).

Establishment of a Tg mouse model constitutively expressing APOBEC2

To investigate the enzymatic activity of APOBEC2 *in vivo*, we generated a Tg mouse model with constitutive and ubiquitous expression of APOBEC2 under the control of CAG promoter. APOBEC2 Tg mice were born healthy and with a body weight similar to that of their wild-type littermates. The expression level of APOBEC2 in various organs of the Tg mice was examined by quantitative RT-PCR and compared with that in the wild-type mice. In wild-type mice, endogenous APOBEC2 transcript was expressed at high levels in heart and skeletal muscle, whereas little or no APOBEC2 expression was detected in the liver, gastrointestinal tracts, lung, spleen and kidney. In contrast, high expression of *APOBEC2* mRNA was ubiquitously detected in the Tg mice, but the expression levels of *APOBEC2* in the liver or lung of the Tg mice were relatively lower than those of the wild-type heart or skeletal muscle (Fig. 2*a*). Immunoblotting analysis using the specific antibodies against APOBEC2 also revealed widespread expression of APOBEC2 protein in various epithelial organs of the Tg mice, with relatively low expression in kidney and spleen (Fig. 2*b*).

Constitutive expression of APOBEC2 resulted in the accumulation of nucleotide alterations in RNA sequences of Eif4g2 and Pten genes in hepatocytes

To clarify whether APOBEC2 targets DNA or RNA, we first extracted total RNA from the nontumor liver tissues of 2 APOBEC2 Tg mice that developed HCC (described below) and their 3 APOBEC2 Tg littermates without any tumor phenotypes, and subjected them to sequence analyses. We chose 2 representative tumor-suppressor genes that are frequently mutated in human cancers, *Pten*, and *Tp53*. The *Bcl6* and *Eif4g2* genes were also included because they are the preferential targets for AID- and APOBEC1-mediated mutagenesis, respectively. We first confirmed that the transcription levels of the genes analyzed for RNA sequencing did not differ between the liver tissues of APOBEC2 Tg mice and wild-type littermates (Supporting Information Fig. S1). In addition, there was no difference in the quantitative levels of APOBEC1 expression between the APOBEC2-expressing liver and

Cancer Cell Biology

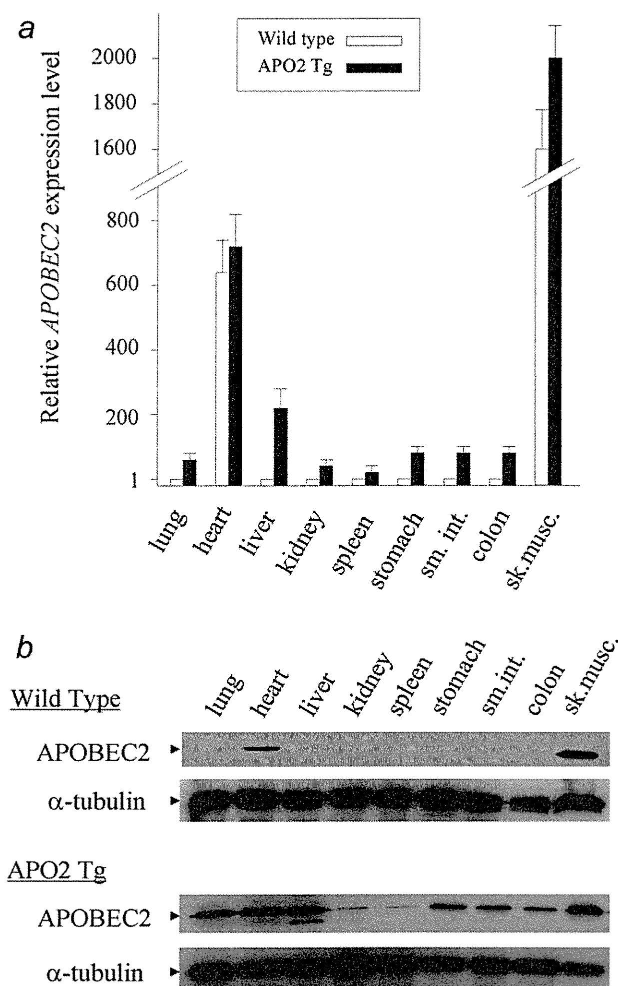

Figure 2. Expression analyses of APOBEC2 Tg mice. (*a*) Relative expression levels of *APOBEC2* transcripts calibrated by the amount of *18S rRNA* for indicated organs of adult APOBEC2 Tg mice (48-week-old) and their wild-type littermates. Data shown are mean results of quantitative real-time RT-PCR analyses for the indicated mouse groups ($n = 6$). Filled bar, APOBEC2 Tg mice; open bar, wild-type mice; sm.int, small intestine; sk.musc, skeletal muscle. (*b*) Results of immunoblot analysis using anti-APOBEC2 (upper panel) or anti-α-tubulin (lower panel) antibody for the lysates of the indicated organs of 48-week-old APOBEC2 Tg mice and their littermates.

normal liver of the wild-type mice (Supporting Information Fig. S2). Sequence analysis revealed a mean of 98,000 and 55,400 base reads per each gene transcript derived from the nontumor liver tissues of the APOBEC2 Tg and control mice, respectively. The total number of amplified clones and RNA sequence reads, and the frequency of nucleotide alterations detected in the nontumor liver tissues of 2 APOBEC2 Tg mice with HCC and the wild-type littermate of the same mouse line are shown in Table 1. The mutation frequencies were highest in the *Eif4g2* transcripts among the genes analyzed in APOBEC2-Tg mice, and were significantly greater compared with those in control tissues (mutation frequencies were 2.75 and 2.36 *vs.* 0.58 substitutions per 1×10^4 nucleotides; $p < 0.05$). Moreover, the nucleotide alteration frequency was significantly higher in the *Pten* gene transcripts from a APOBEC2-expressing liver (Tg-1) than in the control tissues (mutation frequencies were 2.43 *vs.* 0.44 substitutions per 1×10^4 nucleotides, respectively; $p < 0.01$). The *Pten* mRNA of a liver derived from another APOBEC2 Tg mouse (Tg-2; mutation frequency was 1.36 substitutions per 1×10^4 nucleotides) also had a higher nucleotide alteration frequency than that in the control mice, although the difference was not statistically significant ($p = 0.16$ *vs.* control). For the *Eif4g2* and *Pten* transcripts, nucleotide alterations were distributed over the sequences examined and all the alterations detected were different among clones (Fig. 3). Similar results were obtained from the analyses on the liver of 3 APOBEC2 Tg mice that lacked any tumor phenotypes. Indeed, several nucleotide changes had accumulated in both *Eif4g2* and *Pten* transcripts in the liver of all 3 APOBEC2 Tg mice examined (Supporting Information Table S2). In contrast, the mutation frequencies of *Tp53* and *Bcl6* genes of the liver of the APOBEC2 Tg mice were comparable with those of the wild-type mice.

APOBEC2 expression in the liver induced no nucleotide changes in DNA sequences

To clarify whether the nucleotide alterations that emerged in *Eif4g2* and *Pten* transcripts were due to DNA or RNA sequence changes, we determined the DNA sequences of both genes derived from the liver tissues of APOBEC2 Tg and control mice. DNA sequences with an average base length of 0.7 k containing exonic and intronic sequences were amplified, followed by sequence analyses. The total number of amplified clones and DNA sequences read, and the frequency of nucleotide alterations are shown in Supporting Information Table S3. In contrast to the analyses on the RNA sequences, there were no significant differences between the mutation frequency of APOBEC2 Tg mice and that of the wild-type mice of the DNA sequences of the *Eif4g2* and *Pten* genes in the liver. Indeed, no nucleotide alterations were observed in the DNA sequences of the *Eif4g2* gene in the liver of the APOBEC2 Tg mice. Similarly, no mutation was accumulated in the *Pten* DNA sequences of the APOBEC2-expressing liver, suggesting that constitutive expression of the APOBEC2 transgene had no effect on the DNA sequences of the examined regions in the *Eif4g2 and Pten* genes in hepatocytes.

APOBEC2 transgenic mice developed liver and lung tumors

Although most Tg mice were viable at 72 weeks, macroscopic liver and lung tumors developed in some of the APOBEC2 Tg mice. At 72 weeks of age, liver tumors were observed in 2 of 20 Tg male mice, and lung nodules were detected in 7 Tg mice. In contrast to the APOBEC2 Tg mice, none of the wild-type mice developed any tumors at the same age, except 1 with a very small adenoma in the lung. Histopathologic

Table 1. Summary of sequence analysis on the RNA extracted from the liver of the wild-type and APOBEC2 Tg mice

Gene	Mice	Clone	Sequence reads	Nucleotide alterations		
				Number	Frequency(/10^4)	APO2/Wt*
Eif4g2	Wt	82	50,949	3	0.58	
	Tg-1	83	50,835	14	2.75	4.7**
	Tg-2	90	54,986	13	2.36	4.1**
Pten	Wt	92	67,352	3	0.44	
	Tg-1	79	57,599	14	2.43	5.5***
	Tg-2	69	51,323	7	1.36	3.1
Bcl6	Wt	48	41,776	3	0.72	
	Tg-1	59	51,414	1	0.19	0.3
	Tg-2	48	42,413	4	0.94	1.3
Tp53	Wt	84	61,705	2	0.32	
	Tg-1	51	42,285	3	0.71	2.2
	Tg-2	50	40,880	3	0.73	2.3

*Frequency of nucleotide alteration in APOBEC2 Tg mice / in wild type mice. **$p < 0.05$, *vs.* Wt. ***$p < 0.01$, *vs.* Wt.
Abbreviations: Tg, APOBEC2 Tg mice; WT, wild type mice.

analysis of hepatic tumors developed in the APOBEC2 Tg mice revealed nodular aggregates of neoplastic hepatocytes and permeation of tumor cells into residual normal lobules (Fig. 4). Tumor cells had enlarged and hyperchromatic nuclei with chromatin clumping and occasional prominent nucleoli, which were similar to the morphologic characteristics of typical human HCC. On the other hand, lung tumors showed various degrees of cellular atypia, from adenoma to adenocarcinoma (Fig. 5*a*). In addition, monotonous atypical lymphocytes with cytologic features of lymphoblastic lymphoma, such as enlarged round nuclei, irregular nuclear contours, and frequent mitotic figures, massively invaded the spleens of 2 Tg mice (Fig. 5*b*). These findings suggest that constitutive expression of APOBEC2 causes the development of neoplasia in the epithelial organs, including the liver and the lung.

APOBEC2 induced the accumulation of nucleotide alterations of specific target RNA sequences in hepatocytes in vitro

To confirm whether APOBEC2 exerts genotoxic effects on RNA transcripts of the specific target genes, we investigated the alteration frequencies of RNA sequences in cells with constitutive APOBEC2 expression. For this purpose, we established a conditional expression system that allowed for APOBEC2 activation in the cells in response to an estrogen analogue, 4-hydroxytamoxifen (OHT). OHT treatment triggered a posttranslational conformational change and prompt activation of APOBEC2 in APOBEC2-ER expressing cells.[29] We analyzed 3 genes including *PTEN*, *TP53* and *EIF4G2* for the sequence analysis of APOBEC2-mediated mutagenesis *in vitro*. Total RNA was extracted from the APOBEC2-ER expressing HepG2 cells treated with OHT for 8 weeks and the coding RNA sequences of the selected genes were determined by sequence analyses. The total number of amplified clones and RNA sequence reads, and the frequency of nucleotide alterations are shown in Supporting Information Table S4. We found that the emergence of nucleotide alterations in the *PTEN* and *EIF4G2* transcripts was detected at higher frequencies in the cells with APOBEC2 activation compared with control cells treated with OHT, while these differences were not statistically significant ($p = 0.23$ *vs.* control, and $p = 0.39$ *vs.* control, respectively). In contrast, the frequency of nucleotide alterations in the transcripts of the *TP53* in the cells with APOBEC2 activation was comparable with that in the control cells. Similar to the findings obtained from the APOBEC2 Tg mice liver tissues, there were no significant differences between APOBEC2-expressing hepatocytes and control cells in the incidence of nucleotide alterations in the *PTEN* and *EIF4G2* genes (Supporting Information Table S5). These data further suggest that APOBEC2 exerts mutagenic activity in hepatocytes and preferentially achieves nucleotide substitutions in the coding sequences of the specific target genes.

Discussion

Among the APOBEC family members, APOBEC2 and AID homologs can be traced back to bony fish, whereas APOBEC1 and APOBEC3s are restricted to mammals.[30,31] The broad preservation of the APOBEC2 homolog among vertebrates suggests that APOBEC2 has a critical role in the physiology of many species. Little is currently known, however, about the biologic activity of APOBEC2 in any type of cells. Moreover, it is not known whether APOBEC2 possesses nucleotide editing activities like other APOBEC family member proteins. In the present study, we demonstrated for the first time that APOBEC2 expression triggered nucleotide alterations in RNA sequences of the specific genes in hepatocytes. In addition, our findings suggest that APOBEC2 could

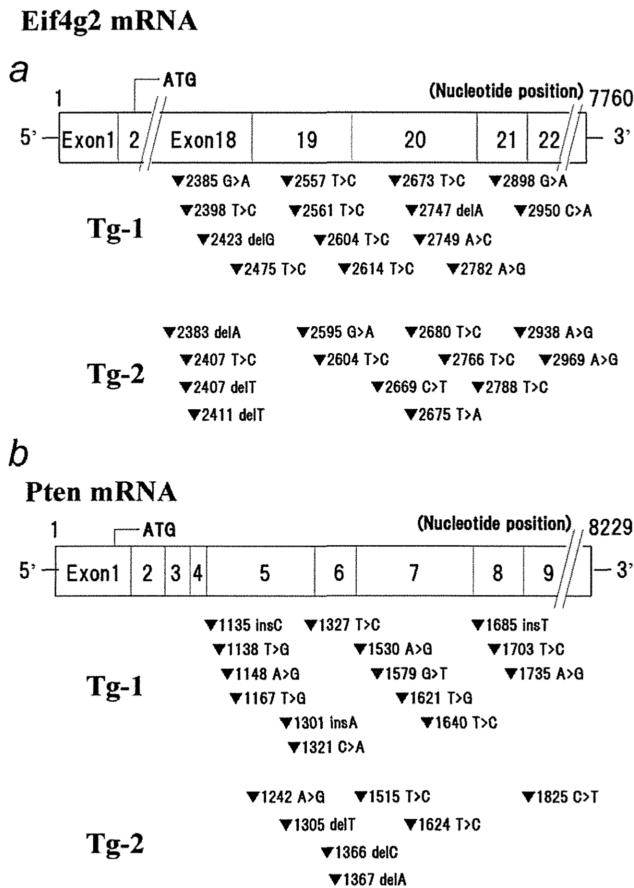

Figure 3. Distribution of nucleotide alterations in the Eif4g2 and Pten trascripts in the APOBEC2-expressing hepatocytes. The mRNA sequences between exon 18 and exon 21 of the Eif4g2 gene (*a*), and the mRNA sequences between exon 5 and exon 8 of the Pten gene (*b*) were determined in the nontumor liver tissues of 2 APOBEC2 Tg mice. The nucleotide positions of the mutations emerged in the Eif4g2 and Pten mRNA of APOBEC2-expressing liver are shown.

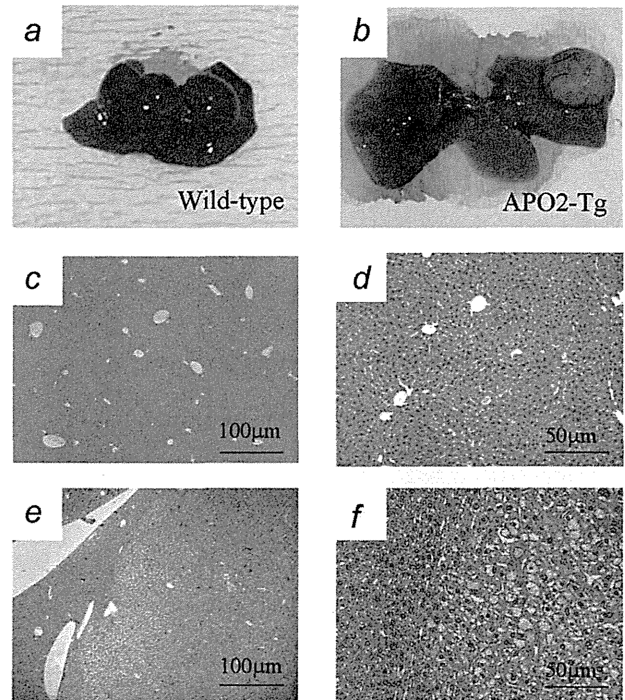

Figure 4. Tumors developed in the liver of APOBEC2 Tg mice. Macroscopic (*b*) and microscopic (haematoxylin and eosin) images (*e, f*) of the HCC that developed in a 72-week-old APOBEC2 Tg mouse and the non-cancerous liver of the same animal (*c,d*). Macroscopic image of the liver of a wild-type littermate is also shown (*a*). (Original magnifications: 3*c,e* ×40; 3*d,f* ×100).

contribute to tumorigenesis via the nucleotide alterations of RNA sequences of the target genes.

On the basis of the close sequence homology of APOBEC2 with other APOBEC proteins, APOBEC2 is thought to exhibit deamination activity to achieve nucleotide editing. Indeed, crystal structure analysis indicates that APOBEC2 contains amino acid residues with 4 monomers in each asymmetric unit that form a tetramer with an atypical elongated shape, and this prominent feature of the APOBEC2 tetramer suggests that the active sites are accessible to large RNA or DNA substrates.[32] In the present study, in a mouse model with constitutive APOBEC2 expression, nucleotide alterations were induced in RNA sequences of the *Eif4g2* and possibly the *Pten* genes in hepatocytes. Similar to its effect *in vivo*, aberrant APOBEC2 expression in cultured hepatocyte-derived cells induced nucleotide alterations in the *EIF4G2* transcripts. Although our findings demonstrate potential mutator activity of the APOBEC2 protein, it is unclear why the *EIF4G2* transcripts were more sensitive to APOBEC2 activity than other genes in hepatocytes. APOBEC1 expression in hepatocytes also induced somatic mutations in the transcripts of the *EIF4G2* gene.[21] Thus, the sequences of the *EIF4G2* gene might be a common target for the nucleotide editing effects of both the APOBEC1 and APOBEC2 proteins. Further analysis is required to identify the specific target genes of APOBEC2-mediated nucleotide editing in hepatocytes.

An intriguing finding was that the mouse model with constitutive and ubiquitous APOBEC2 expression spontaneously developed epithelial neoplasia in the lung and liver tissues as well as lymphoma. Similar phenotypic findings are observed in mouse models expressing APOBEC1 or AID. Tg mice with RNA-editing enzyme APOBEC1 expression develop HCC at high frequencies with an accumulation of somatic mutations at multiple sites on *Eif4g2* mRNA.[20,21] We also demonstrated that AID Tg mice develop tumors in several organs, including the liver, lung, stomach, and the lymphoid tissues through the accumulation of genetic changes induced by the genotoxic effect of AID.[22,23,28] The molecular mechanisms underlying the contribution of constitutive APOBEC2

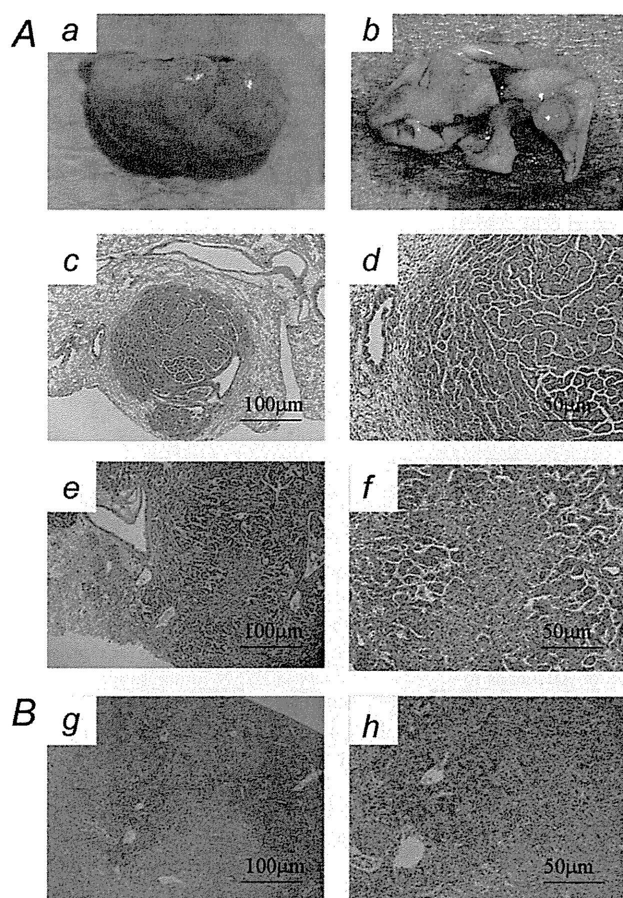

Figure 5. Lung tumors and lymphoma developed in APOBEC2 Tg mice. (*A*) Macroscopic view of a lung tumor that developed in a 72-week-old APOBEC2 Tg mouse (*b*). Microscopic view of a lung adenoma (*c,d*) and adenocarcinoma (*e,f*) that developed in a 72-week-old APOBEC2 Tg mouse. Macroscopic view of the lung of the wild-type littermate (*a*). (*B*) Histologic findings for lymphoma detected in the spleen of APOBEC2 Tg mice. (Original magnifications: 4*c,e,g* ×40; 4*d,f, h* ×100).

expression to tumorigenesis remain unknown. The number of mRNA mutations observed in the *Eif4g2 and Pten* genes in the liver of APOBEC2 Tg mice suggests that these genetic alterations by APOBEC2 have a role in the development of HCC. Indeed, the *EIF4G2* gene is a candidate molecule responsible for oncogenesis caused by the overexpression of APOBEC1,[21] and is frequently downregulated in human cancer tissues.[33] In addition, *PTEN* is one of the most frequently mutated tumor-suppressor genes in human cancers.[34] Thus, the tumorigenesis caused by constitutive APOBEC2 expression might be a consequence of promiscuous nucleotide editing.

Recent studies revealed that the expression of a subset of APOBEC family members is induced by cytokine stimulation in liver tissues. For example, we and other investigators demonstrated that APOBEC3G expression is triggered by interferon-α in hepatocytes, suggesting that APOBEC3G acts as a host defense in response to interferon signaling against viral infection.[35–37] In this study, we showed that TNF-α induced APOBEC2 protein expression in human hepatocytes. Considering the fact that chronic inflammation has important roles in human HCC development,[38,39] the finding that APOBEC2 is induced by proinflammatory cytokine stimulation and induces nucleotide alterations in tumor-related genes in hepatocytes provides a novel idea that aberrant expression of APOBEC2 in epithelial cells acts as a genotoxic factor linking inflammation and cancer development. The tumorigenic phenotype of the APOBEC2-Tg mice further suggests that APOBEC2 is involved in carcinogenesis of the liver tissue under conditions of chronic inflammation, the typical procancerous background of human HCC.

In conclusion, our findings provide the first direct evidence that APOBEC2 induces nucleotide changes preferentially in the *Eif4g2* and possibly the *Pten* genes, and the constitutive expression of APOBEC2 in epithelial tissues contributes to the development of various tumors including HCC and lung cancers. Understanding the pathologic role of APOBEC2 provides new insight into the mechanisms of cancer development in the liver underlying chronic inflammation. During our manuscript preparation, Sato *et al.* reported that they could not find the evidence of APOBEC2's affinity for RNA or high-stoichiometry association with a partner which usually associated with the known RNA editing enzymes.[40] Thus, further analyses would be required to clarify whether APOBEC2 dose possess an RNA-editing activity against specific target genes or overexpression of APOBEC2 causes nucleotide alterations in genome senquences in a promiscuous manner in hepatocytes.

References

1. Wedekind JE, Dance GS, Sowden MP, Smith HC. Messenger RNA editing in mammals: new members of the APOBEC family seeking roles in the family business. *Trends Genet* 2003;19:207–16.
2. Cascalho M. Advantages and disadvantages of cytidine deamination. *J Immunol* 2004; 172:6513–8.
3. Conticello SG, Thomas CJ, Petersen-Mahrt SK, Neuberger MS. Evolution of the AID/APOBEC family of polynucleotide (deoxy)cytidine deaminases. *Mol Biol Evol* 2005;22:367–77.
4. OhAinle M, Kerns JA, Malik HS, Emerman M. Adaptive evolution and antiviral activity of the conserved mammalian cytidine deaminase APOBEC3H. *J Virol* 2006;80:3853–62.
5. Pham P, Bransteitter R, Goodman MF. Reward versus risk: DNA cytidine deaminases triggering immunity and disease. *Biochemistry* 2005;44:2703–15.
6. Chen SH, Habib G, Yang CY, Gu ZW, Lee BR, Weng SA, Silberman SR, Cai SJ, Deslypere JP, Rosseneu M, *et al.* Apolipoprotein B-48 is the product of a messenger RNA with an organ-specific in-frame stop codon. *Science* 1987;238:363–6.
7. Powell LM, Wallis SC, Pease RJ, Edwards YH, Knott TJ, Scott J. A novel form of tissue-specific RNA processing produces apolipoprotein-B48 in intestine. *Cell* 1987; 50:831–40.

8. Mangeat B, Turelli P, Caron G, Friedli M, Perrin L, Trono D. Broad antiretroviral defence by human APOBEC3G through lethal editing of nascent reverse transcripts. *Nature* 2003;424:99–103.
9. Zhang H, Yang B, Pomerantz RJ, Zhang C, Arunachalam SC, Gao L. The cytidine deaminase CEM15 induces hypermutation in newly synthesized HIV-1 DNA. *Nature* 2003;424:94–8.
10. Harris RS, Bishop KN, Sheehy AM, Craig HM, Petersen-Mahrt SK, Watt IN, Neuberger MS, Malim MH. DNA deamination mediates innate immunity to retroviral infection. *Cell* 2003;113:803–9.
11. Shindo K, Takaori-Kondo A, Kobayashi M, Abudu A, Fukunaga K, Uchiyama T. The enzymatic activity of CEM15/Apobec-3G is essential for the regulation of the infectivity of HIV-1 virion but not a sole determinant of its antiviral activity. *J Biol Chem* 2003;278:44412–6.
12. Takaori-Kondo A. APOBEC family proteins: novel antiviral innate immunity. *Int J Hematol* 2006;83:213–6.
13. Noguchi C, Ishino H, Tsuge M, Fujimoto Y, Imamura M, Takahashi S, Chayama K. G to A hypermutation of hepatitis B virus. *Hepatology* 2005;41:626–33.
14. Suspene R, Guetard D, Henry M, Sommer P, Wain-Hobson S, Vartanian JP. Extensive editing of both hepatitis B virus DNA strands by APOBEC3 cytidine deaminases in vitro and in vivo. *Proc Natl Acad Sci USA* 2005;102:8321–6.
15. Noguchi C, Hiraga N, Mori N, Tsuge M, Imamura M, Takahashi S, Fujimoto Y, Ochi H, Abe H, Maekawa T, Yatsuji H, Shirakawa K, *et al.* Dual effect of APOBEC3G on Hepatitis B virus. *J Gen Virol* 2007;88:432–40.
16. Muramatsu M, Sankaranand VS, Anant S, Sugai M, Kinoshita K, Davidson NO, Honjo T. Specific expression of activation-induced cytidine deaminase (AID), a novel member of the RNA-editing deaminase family in germinal center B cells. *J Biol Chem* 1999;274:18470–6.
17. Muramatsu M, Kinoshita K, Fagarasan S, Yamada S, Shinkai Y, Honjo T. Class switch recombination and hypermutation require activation-induced cytidine deaminase (AID), a potential RNA editing enzyme. *Cell* 2000;102:553–63.
18. Liao W, Hong SH, Chan BH, Rudolph FB, Clark SC, Chan L. APOBEC-2, a cardiac- and skeletal muscle-specific member of the cytidine deaminase supergene family. *Biochem Biophys Res Commun* 1999;260: 398–404.
19. Mikl MC, Watt IN, Lu M, Reik W, Davies SL, Neuberger MS, Rada C. Mice deficient in APOBEC2 and APOBEC3. *Mol Cell Biol* 2005;25:7270–7.
20. Yamanaka S, Balestra ME, Ferrell LD, Fan J, Arnold KS, Taylor S, Taylor JM, Innerarity TL. Apolipoprotein B mRNA-editing protein induces hepatocellular carcinoma and dysplasia in transgenic animals. *Proc Natl Acad Sci USA* 1995;92: 8483–7.
21. Yamanaka S, Poksay KS, Arnold KS, Innerarity TL. A novel translational repressor mRNA is edited extensively in livers containing tumors caused by the transgene expression of the apoB mRNA-editing enzyme. *Genes Dev* 1997;11: 321–33.
22. Morisawa T, Marusawa H, Ueda Y, Iwai A, Okazaki IM, Honjo T, Chiba T. Organ-specific profiles of genetic changes in cancers caused by activation-induced cytidine deaminase expression. *Int J Cancer* 2008;123:2735–40.
23. Okazaki IM, Hiai H, Kakazu N, Yamada S, Muramatsu M, Kinoshita K, Honjo T. Constitutive expression of AID leads to tumorigenesis. *J Exp Med* 2003;197: 1173–81.
24. Matsumoto T, Marusawa H, Endo Y, Ueda Y, Matsumoto Y, Chiba T. Expression of APOBEC2 is transcriptionally regulated by NF-kappaB in human hepatocytes. *FEBS Lett* 2006;580:731–5.
25. Kou T, Marusawa H, Kinoshita K, Endo Y, Okazaki IM, Ueda Y, Kodama Y, Haga H, Ikai I, Chiba T. Expression of activation-induced cytidine deaminase in human hepatocytes during hepatocarcinogenesis. *Int J Cancer* 2007;120:469–76.
26. Iwai A, Marusawa H, Matsuzawa S, Fukushima T, Hijikata M, Reed JC, Shimotohno K, Chiba T. Siah-1L, a novel transcript variant belonging to the human Siah family of proteins, regulates beta-catenin activity in a p53-dependent manner. *Oncogene* 2004;23: 7593–600.
27. Schroeder T, Just U. Notch signalling via RBP-J promotes myeloid differentiation. *Embo J* 2000;19:2558–68.
28. Endo Y, Marusawa H, Kinoshita K, Morisawa T, Sakurai T, Okazaki IM, Watashi K, Shimotohno K, Honjo T, Chiba T. Expression of activation-induced cytidine deaminase in human hepatocytes via NF-kappaB signaling. *Oncogene* 2007; 26:5587–95.
29. Doi T, Kinoshita K, Ikegawa M, Muramatsu M, Honjo T. De novo protein synthesis is required for the activation-induced cytidine deaminase function in class-switch recombination. *Proc Natl Acad Sci USA* 2003;100:2634–8.
30. Zhao Y, Pan-Hammarstrom Q, Zhao Z, Hammarstrom L. Identification of the activation-induced cytidine deaminase gene from zebrafish: an evolutionary analysis. *Dev Comp Immunol* 2005;29: 61–71.
31. Saunders HL, Magor BG. Cloning and expression of the AID gene in the channel catfish. *Dev Comp Immunol* 2004;28: 657–63.
32. Prochnow C, Bransteitter R, Klein MG, Goodman MF, Chen XS. The APOBEC-2 crystal structure and functional implications for the deaminase AID. *Nature* 2007;445:447–51.
33. Buim ME, Soares FA, Sarkis AS, Nagai MA. The transcripts of SFRP1,CEP63 and EIF4G2 genes are frequently downregulated in transitional cell carcinomas of the bladder. *Oncology* 2005; 69:445–54.
34. Salmena L, Carracedo A, Pandolfi PP. Tenets of PTEN tumor suppression. *Cell* 2008;133:403–14.
35. Tanaka Y, Marusawa H, Seno H, Matsumoto Y, Ueda Y, Kodama Y, Endo Y, Yamauchi J, Matsumoto T, Takaori-Kondo A, Ikai I, Chiba T. Anti-viral protein APOBEC3G is induced by interferon-alpha stimulation in human hepatocytes. *Biochem Biophys Res Commun* 2006;341:314–9.
36. Bonvin M, Achermann F, Greeve I, Stroka D, Keogh A, Inderbitzin D, Candinas D, Sommer P, Wain-Hobson S, Vartanian JP, Greeve J. Interferon-inducible expression of APOBEC3 editing enzymes in human hepatocytes and inhibition of hepatitis B virus replication. *Hepatology* 2006;43: 1364–74.
37. Komohara Y, Yano H, Shichijo S, Shimotohno K, Itoh K, Yamada A. High expression of APOBEC3G in patients infected with hepatitis C virus. *J Mol Histol* 2006;37:327–32.
38. Thorgeirsson SS, Grisham JW. Molecular pathogenesis of human hepatocellular carcinoma. *Nat Genet* 2002;31:339–46.
39. Llovet JM, Burroughs A, Bruix J. Hepatocellular carcinoma. *Lancet* 2003;362: 1907–17.
40. Sato Y, Probst HC, Tatsumi R, Ikeuchi Y, Neuberger MS, Rada C. Deficiency in APOBEC2 leads to a shift in muscle fiber-type, diminished body mass and myopathy. *J Biol Chem* 2009;285:7111–18.

OPEN ACCESS Freely available online PLoS one

Dynamics of Hepatitis B Virus Quasispecies in Association with Nucleos(t)ide Analogue Treatment Determined by Ultra-Deep Sequencing

Norihiro Nishijima[1], Hiroyuki Marusawa[1]*, Yoshihide Ueda[1], Ken Takahashi[1], Akihiro Nasu[1], Yukio Osaki[2], Tadayuki Kou[3], Shujiro Yazumi[3], Takeshi Fujiwara[4], Soken Tsuchiya[4], Kazuharu Shimizu[4], Shinji Uemoto[5], Tsutomu Chiba[1]

1 Department of Gastroenterology and Hepatology, Graduate School of Medicine, Kyoto University, Kyoto, Japan, 2 Department of Gastroenterology and Hepatology, Osaka Red Cross Hospital, Osaka, Japan, 3 Department of Gastroenterology and Hepatology, Tazuke Kofukai Medical Research Institute, Kitano Hospital, Osaka, Japan, 4 Department of Nanobio Drug Discovery, Graduate School of Pharmaceutical Sciences, Kyoto University, Kyoto, Japan, 5 Department of Surgery, Graduate School of Medicine, Kyoto University, Kyoto, Japan

Abstract

Background and Aims: Although the advent of ultra-deep sequencing technology allows for the analysis of heretofore-undetectable minor viral mutants, a limited amount of information is currently available regarding the clinical implications of hepatitis B virus (HBV) genomic heterogeneity.

Methods: To characterize the HBV genetic heterogeneity in association with anti-viral therapy, we performed ultra-deep sequencing of full-genome HBV in the liver and serum of 19 patients with chronic viral infection, including 14 therapy-naïve and 5 nucleos(t)ide analogue(NA)-treated cases.

Results: Most genomic changes observed in viral variants were single base substitutions and were widely distributed throughout the HBV genome. Four of eight (50%) chronic therapy-naïve HBeAg-negative patients showed a relatively low prevalence of the G1896A pre-core (pre-C) mutant in the liver tissues, suggesting that other mutations were involved in their HBeAg seroconversion. Interestingly, liver tissues in 4 of 5 (80%) of the chronic NA-treated anti-HBe-positive cases had extremely low levels of the G1896A pre-C mutant (0.0%, 0.0%, 0.1%, and 1.1%), suggesting the high sensitivity of the G1896A pre-C mutant to NA. Moreover, various abundances of clones resistant to NA were common in both the liver and serum of treatment-naïve patients, and the proportion of M204VI mutants resistant to lamivudine and entecavir expanded in response to entecavir treatment in the serum of 35.7% (5/14) of patients, suggesting the putative risk of developing drug resistance to NA.

Conclusion: Our findings illustrate the strong advantage of deep sequencing on viral genome as a tool for dissecting the pathophysiology of HBV infection.

Citation: Nishijima N, Marusawa H, Ueda Y, Takahashi K, Nasu A, et al. (2012) Dynamics of Hepatitis B Virus Quasispecies in Association with Nucleos(t)ide Analogue Treatment Determined by Ultra-Deep Sequencing. PLoS ONE 7(4): e35052. doi:10.1371/journal.pone.0035052

Editor: Antonio Bertoletti, Singapore Institute for Clinical Sciences, Singapore

Received November 17, 2011; **Accepted** March 8, 2012; **Published** April 16, 2012

Copyright: © 2012 Nishijima et al. This is an open-access article distributed under the terms of the Creative Commons Attribution License, which permits unrestricted use, distribution, and reproduction in any medium, provided the original author and source are credited.

Funding: This work was supported by JSPS Grant-in-aid for Scientific Research 21229009, 23390196, and Health and Labor Science Research Grants (H22-08) and Research on Hepatitis from the Ministry of Health, Labor and Welfare, Japan. (http://mhlw-grants.niph.go.jp/). The funders had no role in study design, data collection and analysis, decision to publish, or preparation of the manuscript.

Competing Interests: The authors have declared that no competing interests exist.

* E-mail: maru@kuhp.kyoto-u.ac.jp

Introduction

Hepatitis B virus (HBV) is a non-cytopathic DNA virus that infects approximately 350 million people worldwide and is a main cause of liver-related morbidity and mortality [1–3]. The absence of viral-encoded RNA-dependent DNA polymerase proofreading capacity coupled with the extremely high rate of HBV replication yields the potential to rapidly generate mutations at each nucleotide position within the entire genome [4]. Accordingly, a highly characteristic nature of HBV infection is the remarkable genetic heterogeneity at the inter- and intra- patient level. The latter case of variability as a population of closely-related but nonidentical genomes is referred to as viral quasispecies [5,6]. It is well recognized that such mutations may have important implications regarding the pathogenesis of viral disease. For example, in chronic infection, G to A point mutation at nucleotide (nt) 1896 in the pre-core (pre-C) region as well as A1762T and G1764A mutations in the core-promoter region are highly associated with HBeAg seroconversion that in general results in the low levels of viremia and consequent clinical cure [7–9]. In contrast, acute infection with the G1896A pre-C mutant represents a high risk for fulminant hepatic failure [10,11]. Although these facts clearly illustrate the clinical implications of certain viral mutation, increasing evidence strongly suggests that

the viral genetic heterogeneity is more complicated than previously thought [12,13].

The major goals of antiviral therapy in patients with HBV infection are to prevent the progression of liver disease and inhibit the development of hepatocellular carcinoma [14]. Oral nucleos(t)ide analogue (NA) have revolutionized the management of HBV infection, and five such antiviral drugs, including lamivudine, adefovir, entecavir, tenofovir, and telbivudine, are currently approved medications [15,16]. These agents are well-tolerated, very effective at suppressing viral replication, and safe, but one of the major problems of NA therapy is that long-term use of these drugs frequently causes the emergence of antiviral drug-resistant HBV due to substitutions at specific sites in the viral genome sequences, which often negates the benefits of therapy and is associated with hepatitis flares and death [16,17]. It is unclear whether viral clones with antiviral resistance emerge after the administration of antiviral therapy or widely preexist among treatment-naïve patients.

There has been a recent advance in DNA sequencing technology [18]. The ultra-deep sequencers allow for massively parallel amplification and detection of sequences of hundreds of thousands of individual molecules. We recently demonstrated the usefulness of ultra-deep sequencing technology to unveil the massive genetic heterogeneity of hepatitis C virus (HCV) in association with treatment response to antiviral therapy [19]. On the other hand, there are a few published studies in which this technology was used to characterize genetic HBV sequence variations [20–22]. Margeridon-Thermet et al reported that the 454 Life Science GS20 sequencing platform provided higher sensitivity for detecting drug-resistant HBV mutations in the serum of patients treated with nucleoside and nucleotide reverse-transcriptase inhibitors [20]. Solmone et al also reported the strong advantage conferred by the same platform to detect minor variants in the serum of patients with chronic HBV infection [21]. Although in these previous studies low-abundant drug-resistant variants were successfully detected, the analyses were focused on the reverse-transcriptase region of circulating HBV in the serum and thus the whole picture of HBV genetic heterogeneity as well as the *in vivo* dynamics of HBV drug resistant variants in response to anti-viral treatment remains to be clarified. Moreover, intrahepatic viral heterogeneity in patients that achieved the clearance of circulating HBV is largely unknown.

By taking the advantage of an abundance of genetic information obtained by utilizing the Illumina Genome Analyzer II (Illumina, San Diego, CA) as a platform of ultra-deep sequencing, we determined the whole HBV sequence in the liver and serum of patients with chronic HBV infection to evaluate viral quasispecies characteristics. Moreover, we investigated the prevalence of rare drug-resistant HBV variants as well as detailed dynamic changes in the viral genetic heterogeneity in association with NA administration. Based on the abundant genetic information obtained by ultra-deep sequencing, we clarified the precise prevalence of HBV clones with G1896A pre-C mutations in association with HBe serostatus in chronically infected patients with or without NA treatment. We also detected a variety of minor drug-resistant clones in treatment-naïve patients and their dynamic changes in response to entecavir administration, demonstrating the potential clinical significance of naturally-occurring drug-resistant mutations.

Materials and Methods

Ethics Statement

The Kyoto University ethics committee approved the study, and written informed consent for participation in this study was obtained from all patients. The study was conducted in accordance with the principles of the Declaration of Helsinki.

Patients

The liver tissues of 19 Japanese patients that underwent living-donor liver transplantation at Kyoto University due to HBV-related liver disease were available for viral genome analyses. These individuals included 13 men and 6 women, aged 41 to 69 years (median, 55.2 years) and all but one were infected with genotype C viruses. Participants comprised 19 patients with liver cirrhosis caused by chronic HBV infection, including 14 antiviral therapy-naïve cases (chronic-naïve cases) and 5 cases receiving NA treatment, with either lamivudine or entecavir (chronic-NA cases) (Table 1). Serum HBV DNA levels were significantly higher in chronic-naïve cases than in chronic NA cases (median serum HBV DNA levels were 5.6, and <2.6 log copies/ml, respectively, Table 1). Liver tissue samples were obtained at the time of transplantation, frozen immediately, and stored at −80°C until use. Serologic analyses of HBV markers, including hepatitis B surface antigen (HBsAg), antibodies to HBsAg, anti-HBc, HBeAg, and antibodies to HBeAg, were determined by enzyme immunoassay kits as described previously [23]. HBV DNA in the serum before transplantation was examined using a polymerase chain reaction (PCR) assay (Amplicor HBV Monitor, Roche, Branchburg, NJ). To examine the dynamics of viral quasispecies in response to anti-HBV therapy, paired serum samples of 14 treatment-naïve patients before and after administration of daily entecavir (0.5 mg/day) were subjected to further analyses on viral genome.

Direct population Sanger sequencing

DNA was extracted from the liver tissue and serum using a DNeasy Blood & Tissue Kit (Qiagen, Tokyo, Japan). To define the consensus reference sequences of HBV in each clinical specimen, all samples were first subjected to direct population Sanger sequencing using the Applied Biosystems 3500 Genetic Analyzer (Applied Biosystems, Foster City, CA). Oligonucleotide primers for the HBV genome were designed to specifically amplify whole viral sequences as two overlapping fragments using the sense primer 169_F and antisense primer 2847_R to yield a 2679-bp amplicon (amplicon 1), and the sense primer 685_F and antisense primer 443_R to yield a 2974-bp amplicon (amplicon 2; Table S1). HBV sequences were amplified using Phusion High-Fidelity DNA polymerase (FINZYMES, Espoo, Finland). All amplified PCR products were purified using the QIAquick Gel Extraction kit (Qiagen) after agarose gel electrophoresis and used for direct sequencing. The serum of a healthy HBV DNA-negative volunteer was used as a negative control.

Viral genome sequencing by massively-parallel sequencing

Massively-parallel sequencing with multiplexed tags was performed using the Illumina Genome Analyzer II as described [19]. The end-repair of DNA fragments, addition of adenine to the 3′ ends of DNA fragments, adaptor ligation, and PCR amplification by Illumina PCR primers were performed as described previously [24]. Briefly, the viral genome sequences were amplified by high-fidelity PCR using oligonucleotide primers as described above, sheared by nebulization using 32 psi N2 for 8 min, and then the sheared fragments were purified and concentrated using a QIAquick PCR purification Kit (Qiagen). Nucleotide overhangs resulting from fragmentation were then converted into blunt ends using T4 DNA polymerase and Klenow

Table 1. Characteristics of patients with chronic HBV infection analyzed in this study.

	Chronic-naïve (N = 14)	Chronic-NA (N = 5)
Age[†]	55.5 (41–69)	55.0 (49–68)
Sex (male/female)	9/5	4/1
Alanine aminotransaminase (IU/l)[†]	41 (10–74)	30 (15–65)
Total bilirubin (mg/dl)[†]	0.9 (0.5–31.1)	1.7 (0.6–4.5)
Platelet count ($\times10^4$/mm^3)[†]	12.7 (3.3–27.6)	5.1 (3.6–11.3)
HBV genotype		
B	1	0
C	13	5
Viral load (log copies /ml)[†]	5.6 (<2.6–8.8)*	<2.6 (<2.6–5.3)*
HBe-serostatus (HBeAg+/HBeAb+)	8/6	0/5
Fibrosis		
F0–F2	6	0
F3–F4	8	5
Activity		
A0–A1	7	3
A2–A3	7	2

†Values are median (range).
*P = 0.042.
doi:10.1371/journal.pone.0035052.t001

enzymes, followed by the addition of terminal 3′ A-residues. An adaptor containing unique 6-bp tags, such as "ATCACG" and "CGATGT" (Multiplexing Sample Preparation Oligonucleotide Kit, Illumina), was then ligated to each fragment using DNA ligase. We then performed agarose gel electrophoresis of adaptor-ligated DNAs and excised bands from the gel to produce libraries with insert sizes ranging from 200 to 350 bp. These libraries were amplified independently using a minimal PCR amplification step of 18 cycles by Illumina PCR primers with Phusion High-Fidelity DNA polymerase. The DNA fragments were then purified with a MinElute PCR Purification Kit (Qiagen), followed by quantification using the NanoDrop 2000C (Thermo Fisher Scientific, Waltham, MA) to make a working concentration of 10 nM. Cluster generation and sequencing was performed for 64 cycles on the Illumina Genome Analyzer II according to the manufacturer's instructions. The obtained images were analyzed and base-called using GA pipeline software version 1.4 with the default settings provided by Illumina.

Genome Analyzer sequence data analysis

Using the high performance alignment software "NextGene" (SoftGenetics, State College, PA), the 64 base-pair reads obtained from the Genome Analyzer II were aligned with the reference sequences of 3215 bp that were determined by direct population Sanger sequencing of each clinical specimen. Reads with 90% or more bases matching a particular position of the reference sequences were aligned. Furthermore, two quality filters were used for sequencing reads: the reads with a median quality score of more than 30 and no more than 3 uncalled nucleotides were allowed anywhere in the 64 bases. Only sequences that passed the quality filters, rather than raw sequences, were analyzed and each position of the viral genome was assigned a coverage depth, representing the number of times the nucleotide position was sequenced.

Allele-specific quantitative real-time PCR and semiquantitative PCR to determine the relative proportion of G1896A pre-C mutant

To determine the relative proportion of the G1896A pre-C mutant, allele-specific quantitative real-time PCR was performed based on the previously described method [25,26]. Oligonucleotide primers were designed individually to amplify the pre-C region of wild-type and the G1896A pre-C mutant HBV. Three primers were used for this protocol, two allele-specific sense primers, 1896WT_F (for wild-type) and 1896MT_F (for the G1896A pre-C mutant), and one common antisense primer, 2037_R (Table S1). Quantification of wild-type and the G1896A pre-C mutant was individually performed by real-time PCR using a Light Cycler 480 and Fast Start Universal SYBR Master (Roche, Mannheim, Germany) [27]. The relative proportion of the G1896A pre-C mutant was determined to calculate the G1896A pre-C mutant/total HBV ratios. Performance of this assay was tested using mixtures of two previously described plasmids, pcDNA3-HBV-wt#1 and pcDNA3-HBV-G1896A pre-C mutant [28]. Semiquantitative PCR was performed using primers described above, then agarose gel electrophoresis was performed.

Statistical analysis

Results are expressed as mean or median, and range. Pretreatment values were compared using the Mann-Whitney U-test or the Kruskal Wallis H-test. *P* values less than 0.05 were considered statistically significant.

The viral quasispecies characteristics were evaluated by analyzing the genetic complexity based on the number of different sequences present in the population. Genetic complexity for each site was determined by calculating the Shannon entropy using the following formula:

$$Sn = -\frac{\sum_{i=1}^{n} fi(lnfi)}{N}$$

where n is the number of different species identified, fi is the observed frequency of a particular variant in the quasispecies, and N is the total number of clones analyzed [12,13]. The mean viral complexity in each sample was determined by calculating the total amounts of the Shannon entropy at each nucleotide position divided by the total nucleotide number (e.g., 3215 bases) of each HBV genome sequence.

Nucleotide sequence accession number

All sequence reads have been deposit in DNA Data Bank of Japan Sequence Read Archive (http://www.ddbj.nig.ac.jp/index-e.html) under accession number DRA000435.

Results

Validation of multiplex ultra-deep sequencing of the HBV genome

To differentiate true mutations from sequencing errors in the determined sequences, we first generated viral sequence data from the expression plasmid, pcDNA3-HBV-wt#1, encoding wild-type genotype C HBV genome sequences [28]. For this purpose, we determined the PCR-amplified HBV sequences derived from the expression plasmid using high-fidelity Taq polymerase to take the PCR-induced errors as well as sequencing errors into consideration. Viral sequences determined by the conventional Sanger method were used as reference sequences for aligning the amplicons obtained by ultra-deep sequencing. Three repeated ultra-deep sequencing generated a mean of 77,663 filtered reads, corresponding to a mean coverage of 38,234 fold at each nucleotide site (Table S2). Errors comprised insertions (0.00003%), deletions (0.00135%), and nucleotide mismatches (0.037%). The mean overall error rate was 0.034% (distribution of per-nucleotide error rate ranged from 0 to 0.13%) for the three control experiments, reflecting the error introduced by high-fidelity PCR amplification and by multiplex ultra-deep sequencing that remained after filtering out problematic sequences. We also confirmed that multiplex ultra-deep sequencing with and without the high-fidelity PCR amplification with HBV-specific primer sets showed no significant differences in the error rates on the viral sequence data (mean error rate 0.034% vs 0.043%). Accordingly, we defined the cut-off value in its current platform as 0.3%, a value nearly 1 log above the mean overall error rate.

Next, we performed additional control experiments to verify the detectability of the low abundant mutations that presented at a frequency of less than 0.3%. For this purpose, we introduced expression plasmids with a single-point mutation within that encoding a wild-type viral sequence with a ratio of 1:1000 and assessed the sensitivity and accuracy of quantification using high-fidelity PCR amplification followed by multiplex ultra-deep sequencing in association with the different coverage numbers (Table S3). Repeated control experiments revealed that the threshold for detecting low-abundant mutations at an input ratio of 0.10% among the wild-type sequences ranged between 0.11% and 0.24%, indicating that there was no significant difference in the detection rate or error rates under the different coverage conditions. Based on these results, the accuracy of ultra-deep sequencing in its current platform for detecting low-level viral mutations was considered to be greater than 0.30%.

Viral complexity of the HBV quasispecies in association with clinical status

To clarify HBV quasispecies in association with clinical status, we performed multiplex ultra-deep sequencing and determined the HBV full-genome sequences in the liver and serum with chronic HBV infection. First, we compared the sequences of the viral genome determined in the liver tissue with those in the serum and found no significant differences in the viral population between the liver and serum of the same individual. Indeed, the pattern and distribution of genetic heterogeneity of the viral nucleotide sequences in the liver tissue were similar to those observed in the serum of the same patient (Figure S1), suggesting that a similar pattern of viral heterogeneity was maintained in the liver and serum of patients with chronic HBV infection.

Next, we compared the viral heterogeneity in the liver of chronic-naïve and chronic-NA cases. A mean of 5,962,996 bp nucleotides in chronic-naïve cases and 4,866,783 bp nucleotides in chronic-NA cases were mapped onto the reference sequences, and an overall average coverage depth of 1,855 and 1.514 was achieved for each nucleotide site of the HBV sequences, respectively (Table 2). The frequencies of mutated positions and altered sequence variations detected in each viral genomic region are summarized in Table 2. The overall mutation frequency of the total viral genomic sequences was determined to be 0.87% in chronic-naïve cases and 0.69% in chronic-NA cases. Most genomic changes observed in viral variants were single base substitutions, and the genetic heterogeneity of the viral nucleotide sequences was equally observed throughout the individual viral genetic regions, including the pre-surface (preS), S, pre-core~core (preC-C), and X (Table 2). Consistent with the findings obtained from the viral mutation analyses, the overall viral complexity determined by the Shannon entropy value was 0.047 in chronic-naïve and 0.036 in chronic-NA cases, and the viral complexity was equally observed throughout the individual viral genetic region (Figure 1A). Among chronic-naïve cases, we observed no significant differences in the viral complexity in HBV DNA level, age, or degree of fibrosis (Figure 1B).

High sensitivity of the G1896A pre-C mutant to nucleos(t)ide analogues

Emergence of G1896A mutation in the pre-C region, and A1762T and G1764A mutations in the core-promoter region is well known to be associated with HBe-seroconversion [7–9]. We then evaluated the prevalence of these three mutations in the chronically HBV-infected liver, in association with HBe serologic status and the NA treatment history. In chronic-naive cases, 6 and 8 patients showed the pre- and post- HBeAg seroconversion status, respectively (Table 3). The mean prevalence of the G1896A pre-C mutant in HBeAg-positive cases was lower than that in the HBeAg-negative cases (27.4% and 46.5%, respectively). Importantly, however, 4 of 8 HBeAg-negative cases showed a relatively low prevalence of the G1896A pre-C mutant (Liver #8, #12, #13, #14), and all but one case (Liver #10) showed a high prevalence of the A1762T and G1764A mutations, irrespective of HBe serologic status and NA treatment history (Table 3). These findings suggested that other mutations except G1896A, A1762T and G1764A were also involved in the HBeAg seroconversion status. Notably, liver tissues of all but one (Liver #17) chronic-NA cases showed extremely low levels of the G1896A pre-C mutant (0.0, 0.0, 0.1, and 1.1%), suggesting the high sensitivity of the G1896A pre-C mutant to NA (Table 3).

To confirm the difference of the sensitivity to NA between the wild-type and the G1896A pre-C mutant, we examined the dynamic changes of the relative proportion of the G1896A pre-C mutant in the serum of 14 treatment-naïve patients before and after entecavir administration. Consistent with the findings obtained by ultra-deep sequencing, quantitative real-time PCR revealed that entecavir administration significantly reduced the proportion of the G1896A pre-C mutant in 13 of 14 cases (92.9%)

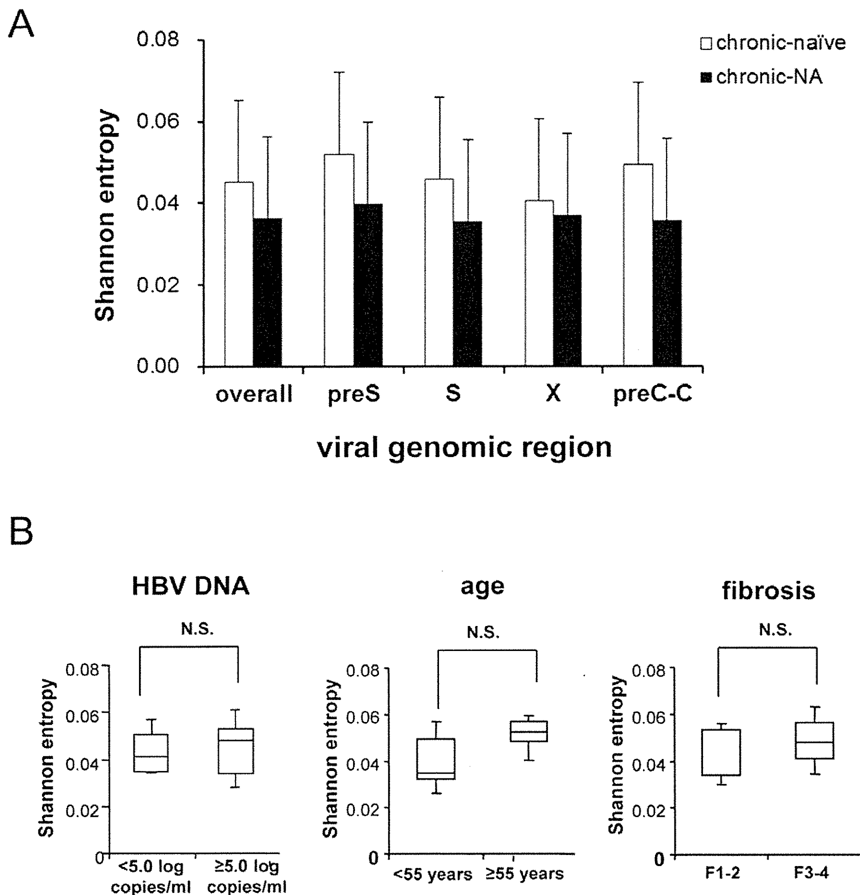

Figure 1. Viral complexity of the HBV quasispecies in association with clinical status. (A) The Shannon entropy values for each viral genomic region were determined in the liver of chronic-naïve and chronic-NA cases. (B) Among the chronic-naïve cases, the Shannon entropy values are shown for patients with serum HBV DNA levels less than 5.0 log copies/ml (<5.0) and greater than 5.0 log copies/ml (≥5.0) (left panel), patients under the age of 55 years (<55) and over the age of 55 (≥55) (middle panel), and patients with low (F1–2) and high (F3–4) liver fibrosis levels (right panel). preS: pre-surface, preC-C: precore~core N.S.: not significant.
doi:10.1371/journal.pone.0035052.g001

Table 2. The frequency of mutation rate and the Shannon entropy in each viral genome region.

	Liver	
	Chronic-naïve (N = 14)	Chronic-NA (N = 5)
Average aligned reads	93,172	76,043
Average aligned nucleotides	5,962,996	4,866,783
Average coverage	1,855	1,514
Mutation rate (%)		
Overall	0.87	0.69
preS	0.92	0.81
S	0.96	0.71
preC-C	1.05	0.72
X	0.63	0.61
Shannon entropy	0.047	0.036

Mutation rate (%): the ratio of total different nucleotides from the reference sequence to total aligned nucleotides.
preS: pre-surface, preC-C: pre-core~core.
doi:10.1371/journal.pone.0035052.t002

irrespective of their HBeAg serostatus, while the G1896A pre-C mutant were detectable in substantial proportion before treatment in all cases (Figure 2A, 2B and 2C; p = 0.001). These results further support the findings that HBV clones comprising the G1896A mutation were more sensitive to NA than those with wild-type sequences.

Prevalence of drug-resistant HBV clones in the liver of treatment-naïve patients

Increasing evidence suggests that drug-resistant viral mutants can be detected in the serum of treatment-naïve patients with chronic HBV infection [20,21]. Thus, we next determined the actual prevalence of spontaneously-developed drug-resistant mutants in chronically-infected liver of treatment-naïve patients to evaluate whether NA treatment potentiates the expansion of drug-resistant clones. The drug-resistant mutations examined included two mutations resistant to lamivudine and entecavir, four mutations resistant to entecavir, and three mutations resistant to adefovir [16,17]. Based on the detection rate of the low-level viral clones determined by the control experiments, we identified the drug-resistant mutants present in each specimen at a frequency of more than 0.3% among the total viral clones. Based on these criteria, at least one resistant mutation was detected in the liver of all of the chronic-naïve cases with chronic HBV infection (Table 4).

Table 3. The prevalence of G1896A mutation in the pre-C region, and A1762T and G1764A mutations in the core-promoter region in the liver of patients chronically infected with HBV.

	HBeAg/HBeAb	NA (duration of treatment)	Mutation Frequency G1896A (Pre C)		A1762T (CP)		G1764A (CP)	
Chronic-naive								
Liver #1	+/−	-	640/1652	(38.7)	1647/1941	(84.9)	1683/1979	(85.0)
Liver #2	+/−	-	9/596	(1.5)	682/687	(99.3)	683/689	(99.1)
Liver #3	+/−	-	273/672	(40.6)	767/769	(99.7)	757/760	(99.6)
Liver #4	+/−	-	204/701	(29.1)	610/625	(97.6)	602/621	(96.9)
Liver #5	+/−	-	27/152	(17.8)	249/250	(99.6)	245/248	(98.8)
Liver #6	+/−	-	228/621	(36.7)	727/729	(99.7)	743/744	(99.9)
Liver #7	−/+	-	740/1193	(62.0)	1908/1913	(99.7)	1888/1913	(98.7)
Liver #8	−/+	-	111/1892	(5.9)	2321/2325	(99.8)	2335/2339	(99.8)
Liver #9	−/+	-	10935/10944	(99.9)	12019/12032	(99.9)	12163/12170	(99.9)
Liver #10	−/+	-	4554/4593	(99.2)	1/5191	(0)	4/5188	(0.1)
Liver #11	−/+	-	811/921	(88.1)	1234/1236	(99.8)	1226/1228	(99.8)
Liver #12	−/+	-	93/1265	(7.4)	1234/1234	(100)	1228/1229	(99.9)
Liver #13	−/+	-	83/877	(9.5)	1465/1529	(95.8)	1485/1549	(95.9)
Liver #14	−/+	-	0/717	(0)	1078/1410	(76.5)	1089/1414	(77.0)
Chronic-NA								
Liver #15	−/+	LAM (156w)	0/390	(0)	441/453	(97.4)	435/448	(97.1)
Liver #16	−/+	ETV (1w)	0/1399	(0)	1624/1632	(99.5)	1625/1630	(99.7)
Liver #17	−/+	LAM (144w)	345/816	(42.3)	988/991	(99.7)	994/994	(100)
Liver #18	−/+	LAM (98w)	2/3963	(0.1)	1015/1188	(85.4)	1190/1194	(99.7)
Liver #19	−/+	LAM (11w)	48/4214	(1.1)	3438/3456	(99.5)	3446/3462	(99.5)

Values in parenthesis show mutation frequency (%): the ratio of total mutant clones to total aligned coverage at each nucleotide sites.
NA: nucleotide analogue, pre C: precore, CP: core promoter, LAM: lamivudine, ETV: entecavir.
doi:10.1371/journal.pone.0035052.t003

The prevalence of the 9 drug-resistant mutations detected by ultra-deep sequencing in 14 chronic-naïve cases ranged from 0.3% to 30.0%, indicating that the proportion of resistant mutations substantially differed in each case. The most commonly detected mutation was M204VI (9 cases) and M250VI (11 cases), which were resistant to lamivudine and entecavir, and entecavir, respectively. Other mutations resistant to adefovir were detected in 7 (50.0%) and 3 (21.4%) cases at A181TV and N236T, respectively (Table 4).

Nine (64.2%) chronic-naïve cases possessed the M204VI mutants in their liver tissues and the proportion of mutant clones among the totally infected viruses ranged from 0.3% to 1.1% among the M204VI mutant-positive patients. In chronic-NA cases, 4 of 5 (80.0%) liver tissues harbored the M204VI mutants with the proportion among the totally infected viruses ranging from 0.4% to 18.7% (Table 4), while the mean serum HBV DNA was suppressed below 2.6 log copies/ml (Table 1). These results suggest that the mutant HBV clones comprising various drug-resistant mutations could latently exist even in the liver of NA treatment-naïve cases.

Expansion of drug-resistant HBV clones harboring M240VI mutations in response to NA administration

To clarify the risk of latent expansion of drug-resistant mutations due to NA treatment, we next examined the early dynamic changes of the prevalence of M204VI mutants in the serum of treatment-naïve patients in response to entecavir treatment. Ultra-deep sequencing provided a mean 40,791- and 38,823-fold coverage of readings, which were mapped to the M204VI nucleotide position at the YMDD sites of each reference sequence in patients before and after entecavir treatment.

Five of 14 (35.7%) patients harbored the M204VI mutations prior to entecavir treatment. Although the serum HBV DNA levels were significantly reduced in response to entecavir in all cases, the M204VI mutant clones were detected in 9 cases (64.3%) after entecavir administration (Table 5). Notably, one patient (Serum #3) who harbored the M240VI mutant clones at baseline had a relatively large expansion of drug-resistant clones among the total viral population in a time-dependent manner in response to entecavir treatment (Table 5). Similarly, M240VI mutant clones became detectable after entecavir administration in four patients (Serum #1, #7, #12, #13) that harbored no resistant mutants at baseline (Table 5). We found no correlation between the degree of the increase in the relative prevalence of M204VI mutant clones and that of the reduction in serum HBV DNA levels. Although only a limited number of patients exhibited a substantial increase in M204VI mutant clones after administration of anti-viral therapy, our findings might suggest that entecavir treatment latently causes selective survival of drug-resistant mutants in treatment naïve patients with chronic HBV infection.

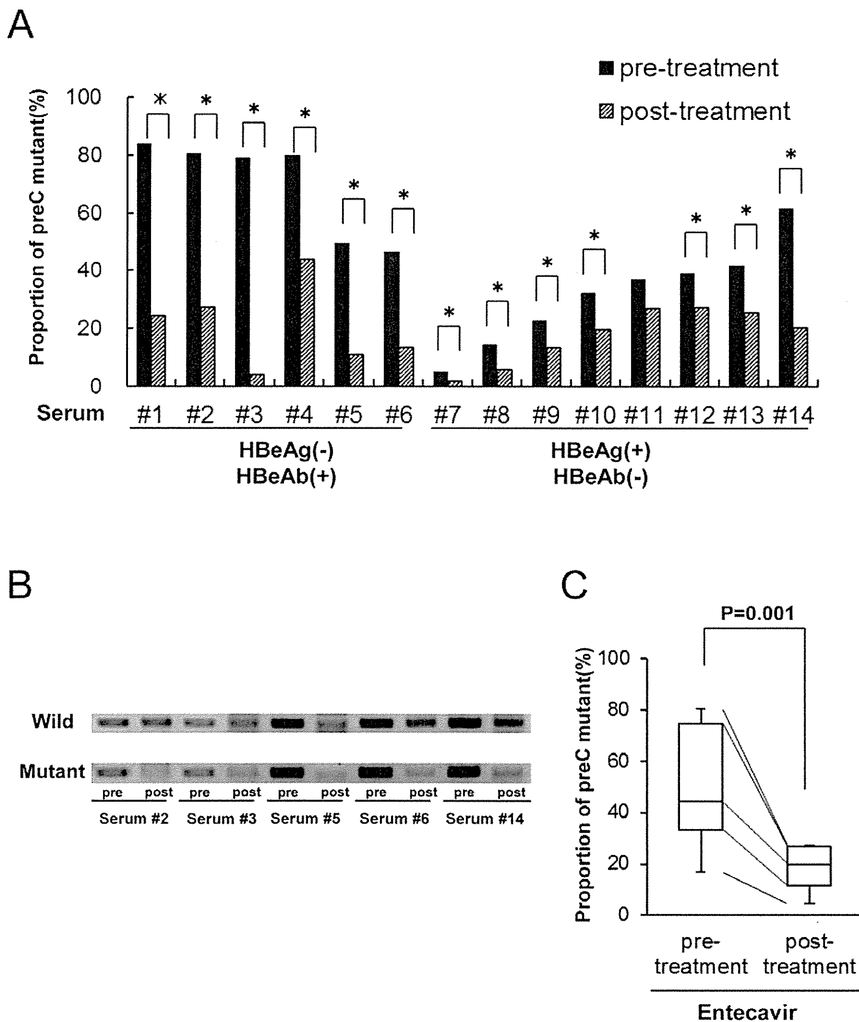

Figure 2. The reduction in the relative proportion of the G1896A pre-C mutant clones after entecavir administration. (A) The relative proportion of the G1896A pre-C mutant was determined in the serum of treatment-naïve patients pre- and post-entecavir administration using quantitative real-time PCR. Serum #1~6 were HBeAg-negative and HBeAb-positive, and Serum #7~14 were HBeAg-positive and HBeAb-negative before treatment. *: $p<0.05$ (B) Semiquantitative PCR analysis was performed using primers specific to the wild-type (upper panel) or G1896A pre-C mutant (lower panel) pre- and post-entecavir administration. A representative result from 5 cases is shown. (C) The relative proportion of the G1896A pre-C mutant was compared in 14 treatment-naïve patients between pre- and post-entecavir administration.
doi:10.1371/journal.pone.0035052.g002

Discussion

Direct population sequencing is the most common method for detecting viral mutations [29]. Conventional sequencing techniques, however, are not efficient for evaluating large amounts of genetic information of the viruses. Newly developed ultra-deep sequencing technology have revolutionized genomic analyses, allowing for studies of the dynamics of viral quasispecies as well as rare genetic variants of the viruses that cannot be detected using standard direct population sequencing techniques [30,31]. The sensitivity of ultra-deep sequencing analysis is primarily limited by errors introduced during PCR amplification and the sequencing reaction, thus it is a challenge to distinguish rare variants from sequencing artifacts. In the present study, we optimized the ultra-deep sequencing with a multiplex-tagging method and reproducibly detected variants within HBV quasispecies that were as rare as 0.3%. Based on this ultra-deep sequencing platform, we determined the abundant genetic heterogeneity of HBV at the intra- and inter-individual levels.

Because of its ability to handle abundant viral genome information, ultra-deep sequencing allowed us to evaluate low-abundant virus variants of patients with chronic HBV infection in detail. It is widely accepted that HBe seroconversion is highly associated with the emergence of G1896A pre-C and/or A1762T and G1764A core promoter mutant clones [7–9]. Unexpectedly, however, our results showed a diverse range of G1896A frequency (0–99.9%) in HBeAg-negative subjects and a high prevalence of core promoter mutations, irrespective of HBe serostatus. Consistent with our observation, previous studies utilizing conventional sequencing methods reported that the frequency of the G1896A pre-C mutant ranged from 12% to 85% [32]. All but one patient (Liver #10) showing a predominance of A1762T and G1764A were infected with genotype C, while patient#10 was infected with genotype B. Because A1762T and G1764A are reported to be significantly more frequent in genotype C [33], the difference in the prevalence of A1762T and G1764A in our study might be a reflection of the viral HBV genotype rather than HBe serostatus. Further investigation of the actual prevalence of these mutations

Table 4. The prevalence of the 9 drug-resistant mutations detected by ultra-deep sequencing derived from liver tissue.

	M204V/I		**L180M**		**T184S/A/I/ L/G/C/M**		**S202C/G/I**		**I169T**	
Drugs	**LAM/ETV**		**LAM/ETV**		**ETV**		**ETV**		**ETV**	
Chronic-naive										
Liver #1	**27/5421**	**(0.5%)**	2/3694	(-)	9/3886	(-)	5/5613	(-)	5/3784	(-)
Liver #2	**35/5344**	**(0.7%)**	0/538	(-)	1/563	(-)	17/6340	(-)	0/512	(-)
Liver #3	**13/1363**	**(1.0%)**	0/304	(-)	1/358	(-)	1/1379	(-)	0/264	(-)
Liver #4	11/5113	(-)	0/556	(-)	**2/547**	**(0.4%)**	11/5133	(-)	0/639	(-)
Liver #5	**2/117**	**(1.1%)**	0/409	(-)	1/380	(-)	1/189	(-)	1/474	(-)
Liver #6	12/8451	(-)	0/309	(-)	0/328	(-)	22/8457	(-)	0/334	(-)
Liver #7	**10/3098**	**(0.3%)**	1/1547	(-)	3/1477	(-)	8/3161	(-)	0/1621	(-)
Liver #8	**13/2442**	**(0.5%)**	1/2378	(-)	6/2312	(-)	1/2564	(-)	1/2507	(-)
Liver #9	**67/13879**	**(0.5%)**	2/5443	(-)	2/5107	(-)	6/13804	(-)	0/5650	(-)
Liver #10	16/7400	(-)	0/3524	(-)	3/3283	(-)	5/7113	(-)	0/3492	(-)
Liver #11	0/412	(-)	1/1328	(-)	**1/295**	**(0.3%)**	0/425	(-)	3/4729	(-)
Liver #12	**4/1098**	**(0.4%)**	1/1389	(-)	0/1272	(-)	2/1102	(-)	0/1544	(-)
Liver #13	**8/2476**	**(0.3%)**	1/2192	(-)	3/2085	(-)	4/2529	(-)	4/5029	(-)
Liver #14	5/3713	(-)	0/2009	(-)	4/1925	(-)	2/3820	(-)	5/3784	(-)
Chronic-NA										
Liver #15	0/339	(-)	0/49	(-)	0/49	(-)	0/338	(-)	0/40	(-)
Liver #16	**28/7278**	**(0.4%)**	0/4403	(-)	6/4053	(-)	14/7556	(-)	6/6084	(-)
Liver #17	**177/945**	**(18.7%)**	0/1059	(-)	0/1009	(-)	0/945	(-)	0/1051	(-)
Liver #18	**13/2655**	**(0.5%)**	0/1239	(-)	0/1185	(-)	**10/2708**	**(0.4%)**	0/1332	(-)
Liver #19	**80/6795**	**(1.2%)**	0/3168	(-)	2/2971	(-)	3/6734	(-)	0/3384	(-)

	M250V/I		**A181T/V**		**N236T**		**P237H**	
Drugs	**ETV**		**ADV**		**ADV**		**ADV**	
Chronic-naive								
Liver #1	**23/2719**	**(0.9%)**	10/3755	(-)	4/4210	(-)	2/4139	(-)
Liver #2	**9/2079**	**(0.4%)**	**2/549**	**(0.4%)**	1/1144	(-)	1/1188	(-)
Liver #3	**10/1699**	**(0.6%)**	**1/298**	**(0.3%)**	3/1636	(-)	1/1666	(-)
Liver #4	**3/388**	**(0.8%)**	**3/549**	**(0.5%)**	0/560	(-)	0/533	(-)
Liver #5	**2/91**	**(2.2%)**	1/409	(-)	0/55	(-)	0/60	(-)
Liver #6	0/214	(-)	**6/305**	**(2.0%)**	**1/294**	**(0.3%)**	0/257	(-)
Liver #7	**7/1289**	**(0.5%)**	4/1531	(-)	**24/2738**	**(0.9%)**	1/2692	(-)
Liver #8	2/1117	(-)	**689/2336**	**(29.5%)**	2/1713	(-)	0/1639	(-)
Liver #9	**27/7325**	**(0.4%)**	**38/5334**	**(0.7%)**	1/6607	(-)	4/6702	(-)
Liver #10	**12/3815**	**(0.3%)**	0/3454	(-)	**13/3245**	**(0.4%)**	2/3272	(-)
Liver #11	**1/199**	**(0.5%)**	1/972	(-)	0/251	(-)	0/251	(-)
Liver #12	**2/672**	**(0.3%)**	**408/1362**	**(30.0%)**	0/598	(-)	0/597	(-)
Liver #13	1/947	(-)	2/2160	(-)	0/1406	(-)	1/1374	(-)
Liver #14	**23/2719**	**(0.9%)**	10/3755	(-)	4/4210	(-)	2/4139	(-)
Chronic-NA								
Liver #15	**1/303**	**(0.3%)**	**2/49**	**(4.1%)**	0/377	(-)	0/384	(-)
Liver #16	1/922	(-)	0/4403	(-)	1/1597	(-)	3/1572	(-)
Liver #17	0/755	(-)	1/1050	(-)	0/698	(-)	**145/698**	**(20.8%)**
Liver #18	1/1464	(-)	2/1206	(-)	0/3156	(-)	0/3107	(-)
Liver #19	8/3834	(-)	**16/3128**	**(0.5%)**	0/3372	(-)	0/3428	(-)

(-): mutant clones less than 0.3% among total clones at each nucleotide sites.
LAM: lamivudine, ADV: adefovir, ETV: entecavir.
doi:10.1371/journal.pone.0035052.t004

Table 5. The prevalence of M204VI mutation at YMDD site in patients before and after entecavir administration.

	Entecavir treatment				
	Before		After		
	Prevalence of the mutated clones		Prevalence of the mutated clones		Period of NA treatment
Serum #3	222/32,238	(0.7%)	2,284/23,791	(9.6%)	2w
Serum #2	401/34,041	(1.2%)	266/25,301	(1.1%)	24w
Serum #5	521/48,723	(1.1%)	245/25,521	(1.0%)	56w
Serum #8	748/65,573	(1.1%)	336/28,702	(1.2%)	48w
Serum #9	312/30,599	(1.0%)	169/14,172	(1.2%)	56w
Serum #1	9/22,843	(-)	2,839/34,162	(8.3%)	8w
Serum #7	26/65,564	(-)	923/66,458	(1.4%)	4w
Serum #12	91/65,616	(-)	258/27,958	(0.9%)	24w
Serum #13	11/23,209	(-)	206/64,747	(0.3%)	32w
Serum #4	3/7,923	(-)	39/65,575	(-)	12w
Serum #6	52/65,582	(-)	77/55,273	(-)	16w
Serum #10	38/22,522	(-)	8/21,053	(-)	8w
Serum #11	47/43,853	(-)	5/16,520	(-)	16w
Serum #14	42/42,784	(-)	40/36,668	(-)	12w

Mutation frequency (%): the ratio of total mutant clones to total aligned coverage at each nucleotide sites.
(-): mutant clones less than 0.3% among total clones at each nucleotide sites.
doi:10.1371/journal.pone.0035052.t005

and the elucidation of other unknown mutations involved in HBe seroconversion are necessary for a better understanding of the underlying mechanisms of HBe seroconversion.

One thing to be noted is that the majority of the chronic-NA cases had extremely low levels of the G1896A pre-C mutant in their liver tissues, even though those cases were serologically positive for anti-HBe and negative for HBeAg. Moreover, entecavir administration significantly reduced the proportion of the G1896A pre-C mutant in the serum of the majority of patients irrespective of their HBeAg serostatus, while the G1896A pre-C mutant clones were detectable in a substantial proportion before treatment in all cases. These findings suggest that the G1896A pre-C mutant have higher sensitivity to NA than the wild-type viruses. Consistent with this hypothesis, several previous studies reported that NA is effective against acute or fulminant hepatitis caused by possible infection with the G1896A pre-C mutant [34,35]. Based on these findings, early administration of NA might be an effective strategy for treating patients with active hepatitis infected predominantly with the G1896A pre-C mutant.

Ultra-deep sequencing has a relatively higher sensitivity than conventional direct population sequencing and is thus useful for detecting drug-resistant mutations not detected by standard sequencing [20,21]. Recently, we revealed that drug-resistant mutants were widely present in treatment-naïve HCV-infected patients, suggesting a putative risk for the expansion of resistant clones to anti-viral therapy [19]. Here, we demonstrated that various drug-resistant HBV variants are present in a proportion of chronically HBV-infected, NA-naïve patients. Several studies using ultra-deep sequencing provided evidence that naturally-occurring drug-resistant mutations are detectable in treatment-naïve individuals with human immunodeficiency virus-1 infection [30,36,37]. Consistent with the cases of human immunodeficiency virus-1 infection, a few studies detected minor variants resistant to NA in the plasma of treatment-naïve patients with chronic HBV infection [20,21]. It remains unclear, however, whether these minor drug-resistant mutations have clinical significance. Our observation of the relative expansion of viral clones with the M204VI mutation during entecavir therapy in some cases indicates the possibility that preexisting minor mutants might provide resistance against NA through the selection of dominant mutant clones. Future studies with a larger cohort size are required to clarify the clinical implications of the latently existing low-abundant drug-resistant mutations.

The current ultra-deep parallel sequencing technology has limitations in the analyses of viral quasispecies. First, because the massively-parallel ultra-deep sequencing platform is based on a multitude of short reads, it is difficult to evaluate the association between nucleotide sites mapped to different genome regions in a single viral clone. Indeed, potential mutational linkages between the pre-C and reverse transcriptase regions were difficult to elucidate due to the short read length of the shotgun sequencing approach. Second, accurate analysis of highly polymorphic viral clones by ultra-deep sequencing is also difficult because the identification of mutations depends strongly on the mapping to the reference genome sequences.

In conclusion, we demonstrated that the majority of patients positive for anti-HBe and negative for HBeAg lacked the predominant infection of the G1896A pre-C mutant in the presence of NA treatment, suggesting that the G1896A pre-C mutant have increased sensitivity to NA therapy compared with wild-type HBV. We also revealed that drug-resistant mutants are widely present, even in the liver of treatment-naïve HBV-infected patients, suggesting that the preexisting low-abundant mutant clones might provide the opportunity to develop drug resistance against NA through the selection of dominant mutations. Further analyses utilizing both novel and conventional sequencing technologies are necessary to understand the significance and clinical relevance of the viral mutations in the pathophysiology of various clinical settings in association with HBV infection.

Supporting Information

Figure S1 Comparison of the viral complexity between the liver and serum of the same individual. Shannon entropy values throughout the whole viral genome of the liver and serum of the representative two cases are shown. (upper two panels, case #11; lower two panels, case #14). preC-C: pre-core~core, preS: pre-surface, P: polymerase.
(TIF)

Table S1 The oligonucleotide primers for amplifying HBV sequences in each clinical specimen.
(DOCX)

Table S2 Error frequency of Ultra-deep sequencing for the expression plasmid encoding wild-type genotype C HBV genome sequences by the three control experiments.
(DOCX)

Table S3 The sensitivity and accuracy of detecting the low abundant minor clones in association with the different coverage numbers.
(DOCX)

Acknowledgments

We thank Prof. G. Tsujimoto, Dr. F. Sato, Dr. Y. Matsumoto, Dr. Y. Endo, Dr. A Takai, Ms. Y. Nakagawa, Ms. K. Fujii and Ms. C. Hirano for ultra-deep sequencing analysis.

Author Contributions

Conceived and designed the experiments: NN HM. Performed the experiments: NN HM. Analyzed the data: NN HM YU AN TF ST KS TC. Contributed reagents/materials/analysis tools: NN HM YU YO TK SY SU. Wrote the paper: NN HM YU KT TC.

References

1. Dienstag JL (2008) Hepatitis B virus infection. N Engl J Med 359: 1486–1500.
2. Lok AS, McMahon BJ (2007) Chronic hepatitis B. Hepatology 45: 507–539.
3. Chang KM (2010) Hepatitis B immunology for clinicians. Clin Liver Dis 14: 409–424.
4. Murray JM, Purcell RH, Wieland SF (2006) The half-life of hepatitis B virions. Hepatology 44: 1117–1121.
5. Ngui SL, Teo CG (1997) Hepatitis B virus genomic heterogeneity: variation between quasispecies may confound molecular epidemiological analyses of transmission incidents. J Viral Hepat 4: 309–315.
6. Hollinger FB (2007) Hepatitis B virus genetic diversity and its impact on diagnostic assays. J Viral Hepat 14 Suppl 1: 11–15.
7. Akahane Y, Yamanaka T, Suzuki H, Sugai Y, Tsuda F, et al. (1990) Chronic active hepatitis with hepatitis B virus DNA and antibody against e antigen in the serum. Disturbed synthesis and secretion of e antigen from hepatocytes due to a point mutation in the precore region. Gastroenterology 99: 1113–1119.
8. Okamoto H, Yotsumoto S, Akahane Y, Yamanaka T, Miyazaki Y, et al. (1990) Hepatitis B viruses with precore region defects prevail in persistently infected hosts along with seroconversion to the antibody against e antigen. J Virol 64: 1298–1303.
9. Kramvis A, Kew MC (1999) The core promoter of hepatitis B virus. J Viral Hepat 6: 415–427.
10. Carman WF, Fagan EA, Hadziyannis S, Karayiannis P, Tassopoulos NC, et al. (1991) Association of a precore genomic variant of hepatitis B virus with fulminant hepatitis. Hepatology 14: 219–222.
11. Omata M, Ehata T, Yokosuka O, Hosoda K, Ohto M (1991) Mutations in the precore region of hepatitis B virus DNA in patients with fulminant and severe hepatitis. N Engl J Med 324: 1699–1704.
12. Domingo E, Gomez J (2007) Quasispecies and its impact on viral hepatitis. Virus Res. Netherlands. pp 131–150.
13. Fishman SL, Branch AD (2009) The quasispecies nature and biological implications of the hepatitis C virus. Infect Genet Evol 9: 1158–1167.
14. Kwon H, Lok AS (2011) Hepatitis B therapy. Nat Rev Gastroenterol Hepatol.
15. Dienstag JL (2009) Benefits and risks of nucleoside analog therapy for hepatitis B. Hepatology 49: S112–121.
16. Ghany MG, Doo EC (2009) Antiviral resistance and hepatitis B therapy. Hepatology 49: S174–184.
17. Zoulim F, Locarnini S (2009) Hepatitis B virus resistance to nucleos(t)ide analogues. Gastroenterology 137: 1593–1608.e1591–1592.
18. Margulies M, Egholm M, Altman WE, Attiya S, Bader JS, et al. (2005) Genome sequencing in microfabricated high-density picolitre reactors. Nature 437: 376–380.
19. Nasu A, Marusawa H, Ueda Y, Nishijima N, Takahashi K, et al. (2011) Genetic heterogeneity of hepatitis C virus in association with antiviral therapy determined by ultra-deep sequencing. PLoS One 6: e24907.
20. Margeridon-Thermet S, Shulman NS, Ahmed A, Shahriar R, Liu T, et al. (2009) Ultra-deep pyrosequencing of hepatitis B virus quasispecies from nucleoside and nucleotide reverse-transcriptase inhibitor (NRTI)-treated patients and NRTI-naive patients. J Infect Dis 199: 1275–1285.
21. Solmone M, Vincenti D, Prosperi MC, Bruselles A, Ippolito G, et al. (2009) Use of massively parallel ultradeep pyrosequencing to characterize the genetic diversity of hepatitis B virus in drug-resistant and drug-naive patients and to detect minor variants in reverse transcriptase and hepatitis B S antigen. J Virol 83: 1718–1726.
22. Han Y, Huang LH, Liu CM, Yang S, Li J, et al. (2009) Characterization of hepatitis B virus reverse transcriptase sequences in Chinese treatment naive patients. J Gastroenterol Hepatol 24: 1417–1423.
23. Ikeda K, Marusawa H, Osaki Y, Nakamura T, Kitajima N, et al. (2007) Antibody to hepatitis B core antigen and risk for hepatitis C-related hepatocellular carcinoma: a prospective study. Ann Intern Med 146: 649–656.
24. Ruike Y, Imanaka Y, Sato F, Shimizu K, Tsujimoto G (2010) Genome-wide analysis of aberrant methylation in human breast cancer cells using methyl-DNA immunoprecipitation combined with high-throughput sequencing. BMC Genomics 11: 137.
25. Louvel S, Battegay M, Vernazza P, Bregenzer T, Klimkait T, et al. (2008) Detection of drug-resistant HIV minorities in clinical specimens and therapy failure. HIV Med 9: 133–141.
26. Ntziora F, Paraskevis D, Haida C, Magiorkinis E, Manesis E, et al. (2009) Quantitative detection of the M204V hepatitis B virus minor variants by amplification refractory mutation system real-time PCR combined with molecular beacon technology. J Clin Microbiol 47: 2544–2550.
27. Matsumoto Y, Marusawa H, Kinoshita K, Endo Y, Kou T, et al. (2007) Helicobacter pylori infection triggers aberrant expression of activation-induced cytidine deaminase in gastric epithelium. Nat Med 13: 470–476.
28. Marusawa H, Matsuzawa S, Welsh K, Zou H, Armstrong R, et al. (2003) HBXIP functions as a cofactor of survivin in apoptosis suppression. EMBO J 22: 2729–2740.
29. Lok AS, Zoulim F, Locarnini S, Bartholomeusz A, Ghany MG, et al. (2007) Antiviral drug-resistant HBV: standardization of nomenclature and assays and recommendations for management. Hepatology 46: 254–265.
30. Hedskog C, Mild M, Jernberg J, Sherwood E, Bratt G, et al. (2010) Dynamics of HIV-1 quasispecies during antiviral treatment dissected using ultra-deep pyrosequencing. PLoS One 5: e11345.
31. Rozera G, Abbate I, Bruselles A, Vlassi C, D'Offizi G, et al. (2009) Massively parallel pyrosequencing highlights minority variants in the HIV-1 env quasispecies deriving from lymphomonocyte sub-populations. Retrovirology 6: 15.
32. Chowdhury A, Santra A, Chakravorty R, Banerji A, Pal S, et al. (2005) Community-based epidemiology of hepatitis B virus infection in West Bengal, India: prevalence of hepatitis B e antigen-negative infection and associated viral variants. J Gastroenterol Hepatol 20: 1712–1720.
33. Orito E, Mizokami M, Sakugawa H, Michitaka K, Ishikawa K, et al. (2001) A case-control study for clinical and molecular biological differences between hepatitis B viruses of genotypes B and C. Japan HBV Genotype Research Group. Hepatology 33: 218–223.
34. Yu JW, Sun LJ, Yan BZ, Kang P, Zhao YH (2011) Lamivudine treatment is associated with improved survival in fulminant hepatitis B. Liver Int 31: 499–506.
35. Lisotti A, Azzaroli F, Buonfiglioli F, Montagnani M, Alessandrelli F, et al. (2008) Lamivudine treatment for severe acute HBV hepatitis. Int J Med Sci 5: 309–312.
36. Simen BB, Simons JF, Hullsiek KH, Novak RM, Macarthur RD, et al. (2009) Low-abundance drug-resistant viral variants in chronically HIV-infected, antiretroviral treatment-naive patients significantly impact treatment outcomes. J Infect Dis 199: 693–701.
37. Lataillade M, Chiarella J, Yang R, Schnittman S, Wirtz V, et al. (2010) Prevalence and clinical significance of HIV drug resistance mutations by ultra-deep sequencing in antiretroviral-naïve subjects in the CASTLE study. PLoS One 5: e10952.

Hepatology Research

Hepatology Research 2013; 43: 67–71 doi: 10.1111/j.1872-034X.2012.01020.x

Original Article

Efficacy and safety of prophylaxis with entecavir and hepatitis B immunoglobulin in preventing hepatitis B recurrence after living-donor liver transplantation

Yoshihide Ueda,[1] Hiroyuki Marusawa,[1] Toshimi Kaido,[2] Yasuhiro Ogura,[2] Kohei Ogawa,[2] Atsushi Yoshizawa,[2] Koichiro Hata,[2] Yasuhiro Fujimoto,[2] Norihiro Nishijima,[1] Tsutomu Chiba[1] and Shinji Uemoto[2]

Departments of [1]Gastroenterology and Hepatology and [2]Surgery, Graduate School of Medicine, Kyoto University, Kyoto, Japan

Aim: Hepatitis B recurrence after liver transplantation can be reduced to less than 10% by combination therapy with lamivudine (LAM) and hepatitis B immunoglobulin (HBIG). The aim of this study was to evaluate the efficacy and safety of prophylaxis with entecavir (ETV), which has higher efficacy and lower resistance rates than LAM, combined with HBIG in preventing hepatitis B recurrence after living-donor liver transplantation (LDLT).

Methods: Twenty-six patients who received ETV plus HBIG (ETV group) after LDLT for hepatitis B virus (HBV)-related end-stage liver disease were analyzed by comparing with 63 control patients who had received LAM plus HBIG (LAM group).

Results: The survival rates of the patients treated with ETV plus HBIG was 73% after both 1 and 3 years, and there was no statistical difference between the patients in the ETV group and LAM group. No HBV recurrence was detected during the median follow-up period of 25.1 months in the ETV group, whereas the HBV recurrence rate was 4% at 3 years and 6% at 5 years in the LAM group. No patients had adverse effects related to ETV administration.

Conclusion: ETV combined with HBIG provides effective and safe prophylaxis in preventing hepatitis B recurrence after LDLT.

Key words: entecavir, hepatitis B, liver transplantation, living donor

INTRODUCTION

THE RECURRENCE OF hepatitis B virus (HBV) infection after liver transplantation for HBV-related diseases resulted in poor outcomes before the development of effective prophylaxis with lamivudine (LAM) and hepatitis B immunoglobulin (HBIG). Without the prophylaxis, the majority of patients developed recurrent infections due to HBV in the early phases after liver transplantation, and the recurrence resulted in rapidly progressive liver injury, early graft loss and reduced survival.[1–3] The development of prophylaxis dramatically reduced the post-transplant recurrence of hepatitis B and markedly improved prognosis. The most widely used prophylaxis so far has been a combination therapy of LAM and i.v. HBIG.

In the non-transplant setting, the long-term use of LAM resulted in high rates of emergence of resistance to the drug, with rates ranging 14–32% after 1 year and 60–70% after 5 years of treatment. In most cases, the resistance was the result of selection of LAM-resistant mutations in the YMDD motif of the DNA polymerase domain of HBV.[4] Moreover, the emergence of HBV strains with mutations that allow escape from hepatitis B surface antibody (anti-HBs) recognition has been reported in patients vaccinated for HBV,[5,6] in patients with chronic hepatitis B[7,8] and in liver transplant recipients after HBIG administration.[9–11] Therefore, the emergence of LAM resistance and HBIG resistance might

Correspondence: Dr Yoshihide Ueda, Department of Gastroenterology and Hepatology, Graduate School of Medicine, Kyoto University, 54 Kawahara-cho, Shogoin, Sakyo-ku, Kyoto 606-8507, Japan. Email: yueda@kuhp.kyoto-u.ac.jp
Received 13 February 2012; revision 6 March 2012; accepted 28 March 2012.

© 2012 The Japan Society of Hepatology

increase the risk of recurrence during long-term administration of LAM and HBIG, although the rate of HBV recurrence in liver transplant recipients who received prophylaxis with LAM and HBIG for more than 10 years has not been reported to date. At present, several nucleoside analogs are available for the treatment of chronic hepatitis B[4]. Among them, there is entecavir (ETV), a carbocyclic analogue of 2′-deoxyguanosine, which has been shown to have higher efficacy than LAM in patients with chronic hepatitis B. In addition, ETV has a higher genetic barrier to resistance than LAM. The resistance to ETV requires at least three mutations including rtM204V/I, which causes LAM-resistance, rtL180M, and a mutation at one of the following codons: rtT184, rtS202 or rtM250.[4] Therefore, ETV is now used as a first-line therapy in the treatment of chronic hepatitis B worldwide. Data available in the published work suggest that, in transplant recipients, ETV plus HBIG represents a better prophylaxis protocol than LAM plus HBIG for long-term prevention of HBV recurrence after liver transplantation. However, the efficacy and safety of this treatment is largely unknown.

The aim of this study was to evaluate the efficacy and safety of prophylaxis with ETV and HBIG in preventing hepatitis B recurrence after living-donor liver transplantation (LDLT).

METHODS

Patients

WE RETROSPECTIVELY ANALYZED the medical records of 97 patients who underwent LDLT for HBV-related end-stage liver diseases from September 2002 to December 2010. Of these, eight patients were excluded from our study because they had breakthrough hepatitis due to HBV with LAM-resistant mutations and were prescribed LAM plus adefovir before liver transplantation. Accordingly, 89 patients were enrolled in this study.

Prophylaxis with ETV or LAM combined with HBIG

Lamivudine plus HBIG therapy was given to all recipients with HBV-related end-stage liver diseases from September 2002 to November 2006, as reported previously.[12] From December 2006, we changed the protocol for prophylaxis to ETV plus HBIG. ETV at a dose of 0.5 mg/day or LAM at a dose of 100 mg/day was given before transplantation, usually when the patient was referred to the hospital and scheduled for transplantation. Preoperative ETV or LAM prophylaxis was followed by combination with HBIG after transplantation. The first application of HBIG at a dose of 200 IU/kg body mass was administrated i.v. during the anhepatic phase of LDLT, and repeated every day for the first 5 days post-surgery. HBV serological markers were examined at weekly intervals for the first 2 months after the transplant, then at monthly intervals, and 1000 IU of HBIG was periodically administrated to maintain the serum anti-HBs titers at more than 500 IU/L during the first 6 months and 200 IU/L thereafter throughout the follow-up period.[12]

Immunosuppression

Tacrolimus and low-dose steroid therapy were administrated to induce immunosuppression in most patients.[13] Mycophenolate mofetil was administrated to patients who experienced refractory rejection or required reduction of tacrolimus dose due to adverse events. Patients who received ABO blood-type-incompatible transplants were treated with rituximab, plasma exchange, and hepatic artery or portal vein infusion with prostaglandin E1 and methylprednisolone.[14]

Diagnosis of HBV activation

Activation of HBV was diagnosed when hepatitis B surface antigens (HBsAg) and/or HBV DNA became positive in the serum of the patients. After LDLT, HBsAg, anti-HBs and serum HBV DNA were measured at least at 3 monthly intervals. Serological HBV markers, including HBsAg, anti-HBs, hepatitis B core antibody, hepatitis B e antigen (HBeAg) and antibodies to HBeAg (anti-HBe), were measured by chemiluminescent enzyme immunoassay (Fuji Rebio, Tokyo, Japan). Serum HBV DNA titer was analyzed using a commercial polymerase chain reaction (PCR) assay (Amplicor HBV Monitor; Roche, Branchburg, NJ, USA). LAM-resistant YMDD mutant virus was detected by the PCR enzyme-linked mini-sequence assay.[15]

Statistical analysis

Baseline characteristics are shown in Table 1. For continuous variables, medians and ranges are given, and the significance of the data was analyzed with the Wilcoxon rank sum test. For categorical variables, counts are given, and the data were analyzed with the χ^2-test. Survival rates and the rates of patients who showed HBV activation after LDLT were estimated using the Kaplan–Meier method and compared using log-rank tests. $P < 0.05$ was considered significant.

© 2012 The Japan Society of Hepatology

Table 1 Baseline characteristics of 90 patients

	Entecavir + HBIG (*n* = 26)	Lamivudine + HBIG (*n* = 63)	*P*-value
Age (years)	55 (33–68)	53 (26–64)	0.062†
Men/women	19/7	46/17	0.995‡
Primary disease			0.595‡
Acute liver failure	6 (23%)	9 (14%)	
Liver cirrhosis, HCC⁻	6 (23%)	20 (32%)	
Liver cirrhosis, HCC⁺	14 (54%)	34 (54%)	
HBV markers before LDLT			
HBsAg⁺	24 (92%)	61 (97%)	0.350‡
HBeAg⁺	6 (23%)	18 (29%)	0.595‡
HBV DNA before LDLT	<2.6 (<2.6–7.6<)	3.7 (<2.6–7.6<)	0.010†
<2.6 log IU/mL	14 (54%)	19 (30%)	0.024‡
Follow-up period (months)	25.1 (0.2–58.6)	70.6 (0.5–109.2)	<0.001†

Qualitative variables are shown in number; and quantitative variables expressed as median (range).
†Wilcoxon rank sum test.
‡χ^2-Test.
HBeAg, hepatitis B e antigen; HBIG, hepatitis B immunoglobulin; HBsAg, hepatitis B surface antigen; HBV, hepatitis B virus; HCC, hepatocellular carcinoma; LDLT, living-donor liver transplantation.

RESULTS

Patient characteristics

TWENTY-SIX PATIENTS who received ETV plus HBIG (ETV group) after LDLT for HBV-related end-stage liver disease were included in this study. Baseline characteristics of these patients are listed in Table 1 and compared with those of 63 control recipients who received LAM plus HBIG (LAM group) at our institute already present in our database. The two groups of patients did not differ significantly by age, sex, primary diseases or serological markers for HBV before LDLT. Serum HBV DNA levels before LDLT were significantly lower in the ETV group than in the LAM group. Fourteen of 26 patients (54%) showed less than 2.6 log IU/mL of serum HBV DNA in the ETV group. Median follow-up period was 25.1 months (range, 0.2–58.6) in the ETV group, whereas it was 70.6 months (range, 0.5–109.2) in the LAM group.

Efficacy and safety of prophylaxis with ETV plus HBIG

Survival rates of the patients treated with ETV plus HBIG estimated by Kaplan–Meier analysis was 73% at both 1 and 3 years (Fig. 1a). There was no difference between the ETV group and the LAM group, in which survival rates were 81% at 1 year, 78% at 3 years and 73% at

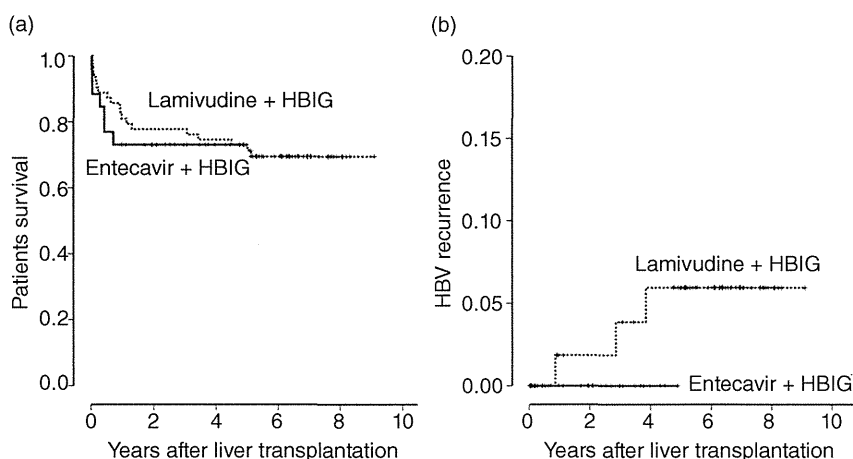

Figure 1 (a) Post-transplantation survival rates and (b) hepatitis B virus (HBV) recurrence after living-donor liver transplantation in HBV positive recipients who received entecavir and hepatitis B immunoglobulin (HBIG) (solid line), or lamivudine and HBIG (dotted line), estimated by Kaplan–Meier method.

© 2012 The Japan Society of Hepatology